VŠB – Technical University of Ostrava

Faculty of Electrical Engineering and Computer Science

BACHELOR'S THESIS

2016 Benjam Wärn

VŠB – Technical University of Ostrava

Faculty of Electrical Engineering and Computer Science

Department of Electrical Power Engineering

Electricity generation from renewable sources
Výroba elektřiny z obnovitelných zdrojů

2016 Benjam Wärn

VŠB - Technical University of Ostrava
Faculty of Electrical Engineering and Computer Science
Department of Electrical Power Engineering

Bachelor Thesis Assignment

Student:	**Benjam Mauritz Wärn**
Study Programme:	B2649 Electrical Engineering
Study Branch:	3907R001 Electrical Power Engineering
Title:	Electricity generation from renewable sources Výroba elektřiny z obnovitelných zdrojů
The thesis language:	English

Description:

o Types of renewable sources (RES).
o Country specific conditions for RES.
o Photovoltaic energy.
o Solar energy.
o Practical measurement.
o Conclusion.

References:

o František Janíček, et al.: Renewable energy sources 1, STU Bratislava 2009, ISBN 978-80-89402-05-2
o Gilbert M. Masters: Renewable and efficient electric power systems, Wiley-IEEE Press 2013, ISBN 978-1-118-14062-8
o Leonard L. Grigsby: Electric power generation, transmission, and distribution, CRC Press 2012, ISBN 978-1-4398-5628-4
o Handbook of Photovoltaic Science and Engineering, Handbook of Photovoltaic Science and Engineering, Second Edition, Edited by Antonio Luque and Steven Hegedus, 2011 John Wiley & Sons, Ltd. ISBN: 978-0-470-72169-8
o http://electrical-engineering-portal.com

Extent and terms of a thesis are specified in directions for its elaboration that are opened to the public on the web sites of the faculty.

Supervisor: **doc. Ing. Radomír Goňo, Ph.D.**

Date of issue: 01.09.2015
Date of submission: 29.04.2016

VYSOKÁ ŠKOLA BÁŇSKÁ-TECHNICKÁ UNIVERZITA Fakulta elektrotechniky a informatiky OSTRAVA 1

prof. Ing. Stanislav Rusek, CSc.
Head of Department

prof. RNDr. Václav Snášel, CSc.
Dean of Faculty

I hereby declare that this bachelor's thesis was written by myself. I have quoted all the references I have drawn upon.

Ostrava, 28 April 2016

Benjam Wärn

Benjam Wärn

ABSTRACT

This thesis covers a basic overview of electricity generation from the most usual renewable energy sources. It gives a further insight into electricity generation from photovoltaics and contain basic formulas and theory concerning photovoltaic cells and panels. It gives an insight into the nature of sunlight from the perspective of photovoltaics.

Further it includes measurements of photovoltaics and a comparison between mono- and polycrystalline panels.

Conclusions are found in the end of the thesis.

Tato bakalářská práce obsahuje základní přehled výroby elektrické energie z nejběžnějších obnovitelných zdrojů. Podrobněji se zabývá výrobou elektřiny z fotovoltaiky a obsahuje základní vztahy a teorii týkající se fotovoltaických článků a panelů. Poskytuje pohled na podstatu slunečního záření z hlediska fotovoltaiky.

Práce dále obsahuje měření fotovoltaických článků a porovnání mezi mono- a polykrystalickými panely.

Závěry jsou formulovány na konci práce.

KEY WORDS

Renewable energy, solar power, photovoltaic, concentrated solar power, power conditioning system, semiconductor, P-N junction, fill factor, maximum power point, irradiance, air mass, volt-ampere characteristic.

Obnovitelná energie, sluneční energie, fotovoltaika, sluneční koncentrátory, systém výkonových kondicionérů, polovodič, P-N přechod, účinnost, bod maximálního výkonu, osvit, hmotnost vzduchu, volt-ampérová charakteristika.

TABLE OF CONTENTS

LIST OF SYMBOLS AND ABBREVIATIONS 8

LIST OF FIGURES AND TABLES 10

INTRODUCTION 11

1. RENEWABLE POWER 12

1.1. Power Sources and Techniques 12
1.1.1. Hydropower 12
1.1.2. Wind power 13
1.1.3. Geothermal heat 13
Dry-steam power stations 14
Flash-steam power stations 14
Binary cycle power stations 14
Enhanced Geothermal Systems (EGS) 14
1.1.4. Bioenergy 15

1.2. Renewable Energy Source Statistics 15

2. SOLAR POWER 17

2.1. Photovoltaics (PV) 17
2.1.1. The photovoltaic cell 17
2.1.2. Semiconductor materials used in photovoltaics 19
Multicrystalline silicon (mc-Si) 19
Single-crystal silicon (sc-Si) 19
Amorphous silicon (a-Si) 19
Cadmium-Telluride (CdTe) 19
2.1.3. Photovoltaic characteristics 19
Volt-ampere characteristics 19
Temperature and irradiance influences 21
2.1.4. Photovoltaic power system 22
Maximum power point tracker (MPPT) 22
Power conditioning system (PCS) 22
Other components 22
Requirements for connection to the grid 23

2.2. Concentrated Solar Power (CSP) 23
2.2.1. Line-focusing CSP systems 24
Parabolic Trough collectors (PTC) 24
Linear Fresnel collectors (LFC) 24

2.2.2. Point-focusing CSP systems 25
Solar Towers (ST) 25
Solar Dishes (SD) 25

2.3. Nature of Sunlight 26
2.3.1. Irradiance 26
2.3.2. Sunlight spectrum 26
2.3.3. Position of the sun 26
2.3.4. PV panel tilt 29
2.3.5. Cloud coverage 30

3. MEASUREMENT OF PHOTOVOLTAICS 31

3.1. Two Photovoltaic Cells SM330 31
3.1.1. PV cell characteristics and inclination influences 31
The setup 31
Results 32
Conclusion 34
3.1.2. Light spectrum influences 35
The setup 35
Results 36
Conclusion 38
3.1.3. Calculation of load resistor size 39
The setup 39
Results 39
Conclusion 39

3.2. Comparison of Mono- and Polycrystalline Photovoltaics 40
3.2.1. PV panel characteristics and inclination influences 40
The setup 40
Results 41
Conclusion 44

CONCLUSION 45

REFERENCES 46

APPENDICES 48

LIST OF SYMBOLS AND ABBREVIATIONS

A	[m^2]	Area
AC		Alternating Current
AM		Air Mass
A_p	[rad]	Azimuth angle of photovoltaic panel
A_s	[rad]	Azimuth angle of sun
a-Si		Amorphous silicon
CdTe		Cadmium-Telluride
CHP		Combined Heat and Power / Cogeneration
CSP		Concentrated Solar Power
DC		Direct Current
d		Number of the day of the year
E	[W/m^2]	Irradiance
e	[C]	Electron charge ($1{,}6021773 \cdot 10^{-19}$C)
EGS		Enhanced Geothermal System
FF		Fill Factor
GTCC		Gas/Steam Turbine Combined Cycle
I	[A]	Current
I_0	[A]	Saturated leakage current
I_{cell}	[A]	Current from photovoltaic cell
I_D	[A]	Current due to recombination
I_{mpp}	[A]	Current at maximum power point
I_{ph}	[A]	Current due to photovoltaic effect
I_{Rsh}	[A]	Current due to shunt resistance
I_{SC}	[A]	Short circuit current
k	[J/K]	Boltzmann constant ($1{,}380658 \cdot 10^{-23}$J/K)
LFC		Linear Fresnel Collector
mc-Si		Multicrystalline silicon
MPP		Maximum Power Point
MPPT		Maximum Power Point Tracker
n		Number of photovoltaic cells connected in series
P	[W]	Power
PCS		Power Conditioning System
P_{mpp}	[W]	Power at maximum power point
PTC		Parabolic Trough Collector
PV		Photovoltaic
PWM		Pulse Width Modulation
REN		Renewables
R	[Ω]	Resistance
R_s	[Ω]	Series resistance
R_{sh}	[Ω]	Shunt resistance
sc-Si		Single-crystal silicon
SD		Solar dish

ST		Solar Tower
STIG		Steam-Injected Gas Turbine
T	[K]	Absolute temperature
T_{UC}	[h]	Coordinated local time
U	[V]	Voltage
U_{cell}	[V]	Cell voltage
U_{mpp}	[V]	Voltage at maximum power point
U_{OC}	[V]	Open circuit voltage
α	[rad]	Angle between perpendicular of photovoltaic panel and sun radiation
δ	[rad]	Declination
ΔU_{sem}	[V]	Voltage between conduction band and valence band
η		Efficiency
λ_e	[rad]	Longitude
ϕ	[rad]	Latitude
ψ_p	[rad]	Elevation angle of photovoltaic panel
ψ_s	[rad]	Elevation angle of sun
ω	[rad]	Hour Angle

LIST OF FIGURES AND TABLES

Figure 1.1 – Total electricity generation in the world from renewables between 2000 and 2012 (5) ...15
Figure 1.2 – REN share in power generation in 2014 in the world (left) (4) and in Finland (right) (6) 16
Figure 2.1 – Photovoltaic cell structure ...18
Figure 2.2 – Equivalent circuit of a PV cell ...18
Figure 2.3 – Volt-ampere- and power characteristics of a photovoltaic ...20
Figure 2.4 – Temperature (left) and irradiance (right) influences on V-A characteristics ...22
Figure 2.5 – Block diagram of photovoltaic power system connected to the grid ...23
Figure 2.6 – Parabolic Trough collector (left) and Linear Fresnel collector (right) ...25
Figure 2.7 – Solar Tower plant (left) and Solar Dishes (right) ...25
Figure 2.8 – Elevation and azimuth in Helsinki, Finland (60°N) ...27
Figure 2.9 – Elevation and azimuth in Rovaniemi, Finland (66°N) ...28
Figure 2.10 – Elevation and azimuth in Prague, Czech Republic (50°N) ...28
Figure 2.11 – Elevation and azimuth angles of the sun and a PV panel ...30
Figure 3.1 – Two photovoltaic cells, Monocrystalline SM330, 0,5V/330mA ...31
Figure 3.2 – Series connection (left) and parallel connection (right) of V-A characteristics measurement with two solar cells SM330 ...32
Figure 3.3 – Setup of V-A characteristics measurement with two solar cells SM330 ...32
Figure 3.4 – Plot of V-A and power characteristics of series connection of two solar cells SM330 for different inclinations ...33
Figure 3.5 – Plot of V-A- and power characteristics of parallel connection of two solar cells SM330 for different inclinations ...33
Figure 3.6 – Relative spectrum of different light sources ...36
Figure 3.7 – Light spectrum influences to photovoltaic SM330 ...38
Figure 3.8 – Resistance compared to power output from solar cells SM330 ...39
Figure 3.9 – Connection diagram of V-A characteristics measurement of PV panels Siemens T10 and Schott Poly 165 ...41
Figure 3.10 – Measurement setup of Monocrystalline panel Siemens T10 (left) and polycrystalline panel Schott Poly 165 (right) ...41
Figure 3.11 – Plot of V-A- and power characteristics of monocrystalline PV panel Siemens T10 for different inclinations ...42
Figure 3.12 – Plot of V-A- and power characteristics of polycrystalline PV panel Schott Poly 165 for different inclinations ...43
Table 3.1 – Irradiance from different lamps ...36

INTRODUCTION

Power production from renewable energy sources are increasing rapidly in times when global warming is becoming a greater issue year after year. Governments are supporting power production from renewable sources and plans are made to decrease the use of fossil fuels. We have already come so far that we cannot stop global warming but we can still influence how strongly it will affect us during the next century.

Lot of research is done to find better, more efficient and reliable ways to produce green power. We have seen lot of success especially in the field of photovoltaics. New, more efficient cells have been made and the production cost of photovoltaics have dropped.

This thesis gives an overview of the most common techniques that are used to produce electricity from renewables and a further insight is given about photovoltaics and solar power. In Chapter 1 a general overview of the most common and mature renewable sources are given and their operation is shortly described. Chapter 2 is dedicated to solar power and photovoltaics, which is the main topic of this thesis. Except of photovoltaics, we also look at CSP systems and at the nature of sun radiation. Chapter 3 cover practical measurements of photovoltaics. Measurements are done on two small photovoltaic cells that are used by students for educational purposes. Further a comparison is made between a monocrystalline and a polycrystalline photovoltaic panel.

1. RENEWABLE POWER

In this chapter we will get an insight into different generation methods from renewable energy sources and look at some statistics of the share of renewables, especially in Finland. Solar power is not included in this chapter since we will get a deeper insight into that in Chapter 2.

1.1. POWER SOURCES AND TECHNIQUES

1.1.1. Hydropower

Conventional hydropower utilize the potential energy in dammed water. The power output from a hydro turbine is proportional to the water flow speed and the *head*, which is the difference in water levels before and after the turbine.

Hydropower plants can be divided according to size, design of station, design of turbine and so on. Division according to size is different between countries but in Finland it is divided as follows (1):

1. Mini, <1 MW
2. Small, 1-10 MW
3. Large, >10 MW

According to design of station, hydropower plants are often divided into:

1. Conventional hydropower or dams
2. Run-of-the-river
3. Pumped storage
4. Tide and wave

The most common design is called *Conventional hydropower*. It includes a dam of water, a storage that can be used according to needs of power generation. Even though there might not be water flowing into the dam or the input water flow to the dam is smaller than the output, the amount of water in the dam is so large that the power station can utilize the dammed water to continue generating electricity. This is not possible with *Run-of-the-river* type. In this design the output power is largely dependent on the input water flow to the power station or the water flow in the river. There is no dam or storage of water that can be used. Therefore the output power from the power station alter more between annual seasons according to the instantaneous water flow in the river.

Pumped storage type is used only for load balancing, to produce electricity during high demand peaks. The idea is to pump water during low demand to a higher potential and later during high demand use the pumped water to produce electricity. Therefore pumped storage is not a source of energy, but a way of balancing load during the day and giving an economical advantage.

There are several different ways how electricity can be generated out of tides or waves. A *Tidal stream generator* takes advantage of the kinetic energy in the tides. Its function is basically the same as for wind turbines but the turbine wings have a smaller diameter than a wind turbine since water has a higher density than air. The turbines are located on the seabed where the water movements are the strongest. A *Tidal barrage* though is used to generate electricity out of the potential energy between high tide and low tide. During low tide water is passed from a higher potential through a hydro turbine to a lower potential to generate electricity. Utilizing wave energy is still only in an experimental stage and there does not yet exist a plant that is connected to the grid. The energy that can be utilized in a

wave is stored half as elevation energy as the height of the wave and the other half as kinetic energy in the wave's forward movement.

There are two types of hydro turbines and several different designs:

1. Impulse turbines
2. Reaction turbines

Impulse turbines are turbines where the turbine is not flooded with water and *nozzles* are used to create a jet of water that turns the turbine. An example of an impulse turbine is the *Pelton turbine* where one or several jets of water turn the runner wheel. *Reaction turbines* on the other hand are flooded with water and the water pressure is higher before the turbine than it is after. This is due to the fact that energy is extracted in the turbine to rotational energy. The most common reaction turbines are the *Kaplan turbine* and the *Francis turbine*. The Kaplan turbine can not only change the pitch of the distribution wheel but also the pitch of the runner blades. Therefore it is advantageous to use the Kaplan turbine in locations with changing head. Francis turbines are suitable for locations with high heads and high water flows. The water is led to the runner through a tapering, spiral tube, which is located around the distribution wheel. After passing through the runner with fixed blades the water leaves the turbine through a tube perpendicular to the intake tube (2).

1.1.2. Wind power

The power extracted from a wind mill is proportional to the cube of the wind speed. Wind in itself is a highly unpredictable source of power and fluctuates a lot in all timescales, from minutes to seasons. These facts result in that the generated power from a wind mill also fluctuates a lot.

Wind turbines can operate within a given range of wind speed. If the wind speed is too low, it will not be enough to produce electricity and therefore the wind turbine will stand. The lower wind speed at which the turbine will stop is called the *cut-in-speed* and it is often at about 3-4m/s. On the other hand if wind speed gets too high, the turbine has to stand as well to protect itself from mechanical failure. The higher wind speed at which the turbine stops is called the *cut-out-speed* and it is often at about 25m/s.

The main parts of a wind mill is the wind turbine and the turbine blades and the generator. The pitch of the blades of the rotor can be adjusted so that the maximum power in the wind can be captured. A multistage gearbox can be used, depending on design, to adjust the rotor speed to match as closely as possible to the grid frequency at every moment for different wind speeds. In other designs an AC/DC/AC converter is used to convert the changing frequency from the generator to a constant frequency that is fed to the grid. It is also possible that the excitation frequency of the rotor in the generator is changed to match the rotor speed so that a constant frequency can be drawn from the generator stator. All of these parts are located in a nacelle, which is mounted on top of a tower. The nacelle can rotate by help of a yaw motor so that the turbine blades are always turned against the wind (3).

1.1.3. Geothermal heat

Geothermal heat can be used to produce electricity and to produce heat for different purposes such as district heating. The heat is carried to the power plant by a heat transfer fluid, usually water or steam from an underground heat reservoir. Geothermal power plants usually provide base load and are

usually located at thermally active areas where hydrothermal reservoirs with naturally high permeability can be found. A technique called *Enhanced Geothermal System* (EGS) can also be used to extract heat from less thermally active locations.

The power plant design depends on the production well heat carrier temperature and pressure. *Cogeneration* (CHP) can be used to increase power plant efficiency and to produce heat for different purposes such as district heating.

Dry-steam power stations
Dry-steam power stations are installed at locations where dry steam can be extracted from the production well. When high-temperature water rises from the thermal reservoir it starts boiling since the pressure decreases. At the production well all the water has become steam and this steam can directly be used to power a steam turbine and generator. This kind of power plants are used at locations with reservoir temperatures of 150 °C or more.

After the steam has passed the steam turbine, some of it has condensed but it still contains a lot of energy that can be used for district heating or other applications where heat is used. Any remaining steam is condensed and pumped back to the reservoir through the injection well to sustain the reservoir capacity.

Flash-steam power stations
Flash-steam power stations usually use reservoirs with slightly lower reservoir temperatures than Dry-steam stations. High-temperature water or steam can be extracted from the production well and a separator is used to separate steam from fluids. The steam is used in the steam turbine and the remaining high temperature fluid can be flashed in a flashing system to a lower pressure so that more steam is extracted and the maximum possible energy can be drawn from the geothermal fluid. Flashing systems can be used successively and several steam turbines can be used to maximize the efficiency.

Binary cycle power stations
Binary cycle plants have separate piping systems for the geothermal fluid and the secondary fluid or steam that runs the turbine. These plants have a reservoir temperature usually between 70°C and 170°C. The geothermal fluid from the production well is used to heat a secondary fluid or a working fluid, such as isopentane or isobutene, since they have low boiling temperatures. This working fluid becomes steam and is used to run the steam turbine and generator. The geothermal fluid is then pumped back to the reservoir through the injection well.

Enhanced Geothermal Systems (EGS)
EGS is a technique used to enhance the extraction of thermal energy from locations with low permeability. A fraction network is created in the reservoir so that water can easily flow between the injection well and the production well. This creates a closed loop for the geothermal fluid through the injection well and the production well. This fact enhances the thermal transition from the reservoir to the geothermal fluid or water that is circulating in the system.

Unlike from hydrothermal reservoirs with high permeability and temperatures, EGS reservoirs have a lower fluid temperature at the production well and they are often used together with a Binary cycle power station.

1.1.4. Bioenergy

There are mainly two different approaches to generate electricity out of biomass. The first approach is direct combustion of biomass such as waste wood in a conventional thermal power plant configuration. The heat produced in the combustion boils water that produces steam, which is subsequently used in a steam turbine.

The second approach is to produce biogas from biomass by using different techniques. Communal waste is often used as biomass in these plants. The gas that is produced is then combusted in a gas turbine similarly as it is in a natural gas power plant. The advantage of the gasification process is that it greatly increases the overall plant efficiency.

Combined designs between steam turbines and gas turbines can be used to further increase the efficiency. Cogeneration can also be used to not only produce electricity but also heat for different purposes. In a *Gas/Steam turbine combined cycle* (GTCC) system the hot combustion gases from the gas turbine are used to produce steam, which is then used in a steam turbine connected to the same generator shaft. Another technique to increase the efficiency is to use a *Steam-injected gas turbine* (STIG) design where the hot exhaust gases from the gas turbine are used to produce water steam that is subsequently forced to the gas turbine to increase the working media in the turbine (2).

1.2. Renewable Energy Source Statistics

Renewable power generation is rapidly growing around the world and in 2014 it represented as much as 58,5 % of capacity additions (4). Hydropower has always been the largest source of renewable power, but during the last five years we have seen a rapid growth of other sources, such as solar power and wind power, as seen in Figure 1.1. In 2014 solar power, which will be discussed later, had a share of 4 % the of generated power by renewables and wind power had a share of 13 %. This can be seen in Figure 1.2. Since solar and wind power are dependent on the weather conditions, the worldwide installed capacity is growing a lot more than the actual generation since renewables are growing so fast. In 2014 the total worldwide installed electric power capacity was about 6,6 TW. Of that was 27,7% renewable sources and they produced 22,8 % of all electricity in the world (4).

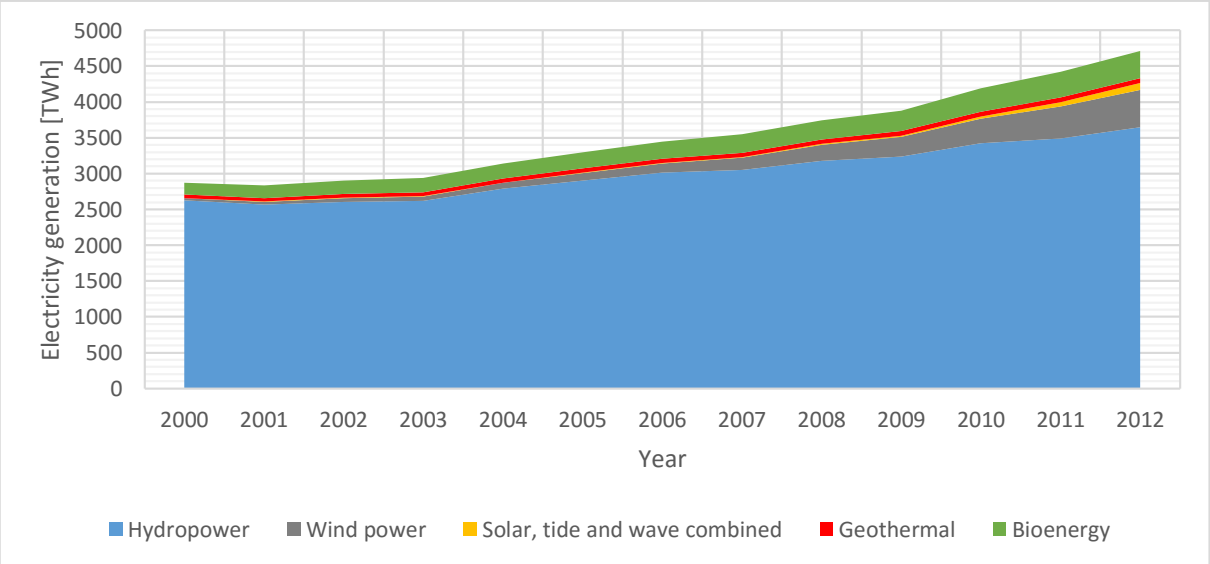

Figure 1.1 – Total electricity generation in the world from renewables between 2000 and 2012 (5)

In Finland the amount of non-renewable energy sources in power generation is decreasing while renewables are increasing. In 2013, 36 % of the generated power was from renewable sources, while in 2014 it was 39 % (6). The sudden increase is due to an increased generation from hydropower in 2014 and a decrease of electricity use in industry (7). Solar power is mainly used in locations where there are no power grid connection, for example at summer cottages. The use of solar power connected to the grid is not that profitable in Finland since about 90 % of the solar radiation is received between March and September (8). This is the situation in the most south of Finland and when going north, the alternation in irradiated power between seasons is even greater. This makes solar power an impractical source of energy, especially for grid connections since the greatest demand for electric power is during winter time when solar radiation is the lowest. Because of this fact, wind power is preferred before solar power in grid connections. Hydropower is the main renewable power source in Finland and in 2014 hydropower produced about 52 % of all the power generated by renewable sources, as seen in Figure 1.2. In 2014 the total generated electric power was 65,4 TWh (6).

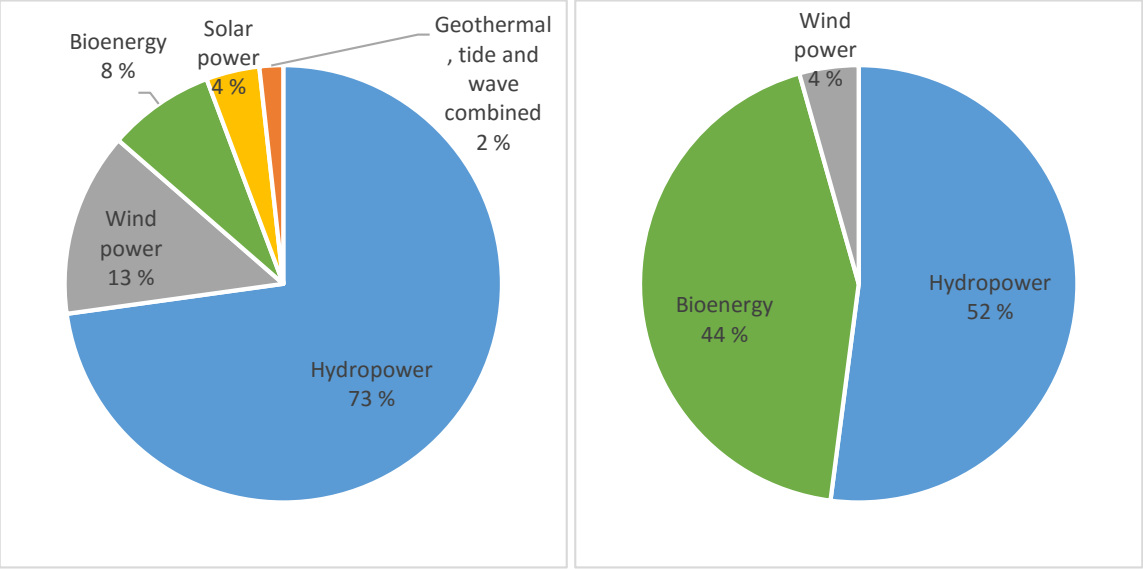

Figure 1.2 – REN share in power generation in 2014 in the world (left) (4) *and in Finland (right)* (6)

For the future Finland has a strict energy policy, one of the strictest in the world. It is planned that Finland would, if needed, by law prohibit the combustion of coal by 2030 and reduce the use of oil by 50 %. The European Union has a plan of cutting CO_2 emissions by 40 % until 2030, but Finland has an own policy of cutting it by 50 %. These goals are planned to be reached by an addition of other renewable sources, such as bioenergy from waste, improving power generation efficiency and reducing energy losses. Other plans that are made to reach the goal is by increasing the use of biofuel by 40 % and increasing the number of electric vehicles to a number of 200 000-300 000 from todays 1 000. (9)

2. SOLAR POWER

In this chapter we will go through the theory of photovoltaics and their operation. Later we will look at different CSP systems and at the nature of sunlight.

There are two main ways of converting the radiation from the sun into useful energy. *Photovoltaics* (PV) can be used to directly convert the radiation into electricity. A technique called *Concentrated Solar Power* (CSP) can be used to indirectly generate electricity. CSP can also be used to generate heat for space heating or district heating. *Solar thermal collectors* can also be used in small scale for space heating or to produce hot water but that topic will not be covered in this thesis.

2.1. PHOTOVOLTAICS (PV)

The radiation from the sun can be captured by a photovoltaic cell to generate an electric current. The voltage that is produced in one PV cell is minimal and therefore PV cells are connected in series to produce a higher voltage. When PV cells are connected in series they create a *PV module*. Several modules connected together make a *PV array* or *PV panel*. Auxiliary electronic equipment is needed to get the highest possible output power from the PV panel, to generate a usable AC voltage or to make it possible to connect the PV panel to the power grid.

We will first get an insight in the physics behind the PV cell and how an electric current is generated by the help of photons in sunlight. Later we will look at typical characteristics for PV cells and how a whole PV power system operates and what is required for a proper operation. In the end of this chapter we will also discuss the nature of sunlight, such as differences in irradiance during different seasons and how the angle of the solar panel towards the sun affects the output power.

2.1.1. The photovoltaic cell

A PV cell is made out of two differently doped semiconductors. The different dopants or impurities are called *donors* or *acceptors* depending on what kind of characteristic they give the semiconductor material. After doping a semiconductor with a donor or an acceptor it becomes a *P-type* or an *N-type* semiconductor. When joining those two semiconductor materials together they create a *P-N junction* or a *depletion region* between the P-type and the N-type semiconductor materials. The P-type semiconductor side is denoted the *valence band* and the N-type semiconductor side is denoted the *conduction band*.

Depending on the semiconductor material that is used, the atoms in the material create different crystalline structures, meaning that the atoms in the material have a periodical, pure structure. This gives semiconductors their electronic properties. Silicon (Si), which is the most common material used in solar cells, has four valence electrons in its atom. Therefore silicon creates a crystalline structure so that every atom has a covalent binding to four other atoms. By adding dopants to this crystalline structure it can be modified so that there is an excess of either *electrons* or *holes*.

When a photon in sun radiation hits the conduction band it goes through it to hit the valence band. This photon thermally excites an electron from the valence band and the electron goes over to the conduction band. This creates a hole or a positively-charged particle in the valence band or the p-type semiconductor and an electron or a negatively-charged particle in the conduction band or the n-type semiconductor. The photon therefore causes a so called *electron-hole pair*. It is these holes and electrons that are the carriers of the electric current.

Only those photons with a greater energy than the semiconductor *bandgap energy* can excite an electron so that it goes over from the valence band to the conduction band leaving a hole behind and creating an electric current. This energy in the photon is dependent on the wavelength of the particle. Therefore the spectral composition of sunlight is an important factor that needs to be taken into account when designing PV cells, so that a maximum amount of wavelengths in sunlight are able to excite electrons in the semiconductor.

Recombination is the term used for the phenomenon where electrons go back to the valence band from their excited state. Figure 2.2 shows the equivalent circuit for a PV cell. Recombination is depicted as the diode with a current I_D. The current or excitation, which is created by the photons, is depicted as the current source with current I_{ph}. It is seen that current I_D has an opposite direction to the generated current I_{ph}. Recombination is therefore a loss in the PV cell that is aimed to be minimized. In the PV cell there are also some shunt resistance, R_{sh} and series resistance, R_s. The current I_{cell} is the current from the PV cell and U_{cell} is the output voltage at the cell terminals.

Other parts that are included in the physical PV cell are conductors on the front and the back of the cell that carry the generated current. On the front, there is an anti-reflective coating so that the maximum amount of light is absorbed by the cell.

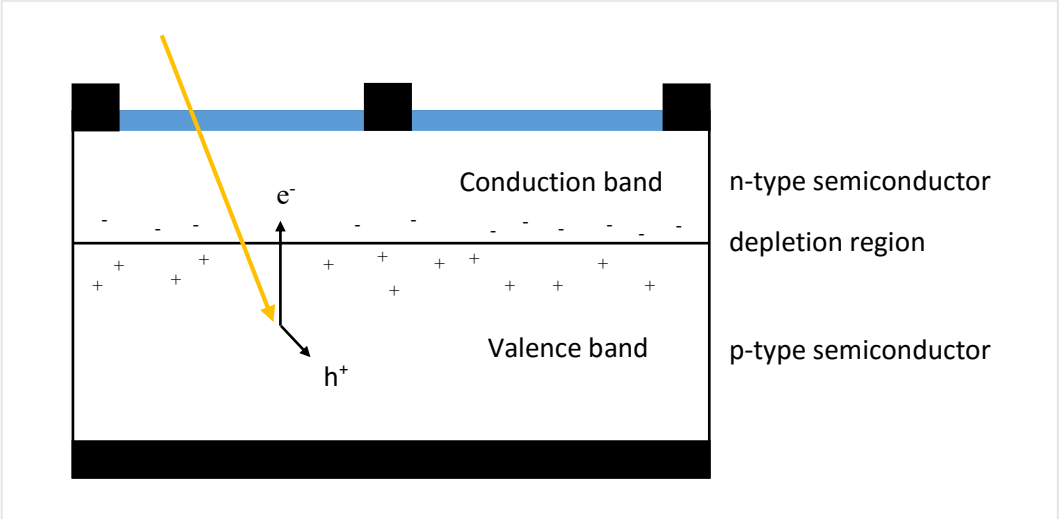

Figure 2.1 – Photovoltaic cell structure

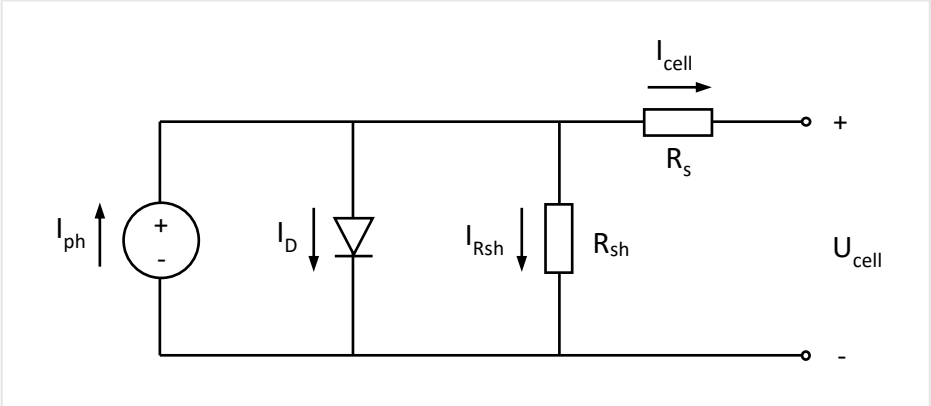

Figure 2.2 – Equivalent circuit of a PV cell

2.1.2. Semiconductor materials used in photovoltaics

Multicrystalline silicon (mc-Si)

Multicrystalline silicon emerged in the 1980s' as an alternative to the expensive single-crystal silicon cells. The efficiency was lower but because of their low price their market still grew.

Mc-Si is a crystalline material but only partly. It creates *grains* where the crystal structure is complete but is broken at the intersection between the grains. The efficiency is slightly smaller than for sc-Si cells but mc-Si PV panels are still the most common ones.

Single-crystal silicon (sc-Si)

Unlike the mc-Si cells, the single-crystal silicon cells have a crystalline structure throughout the whole cell. One PV cell is basically one big silicon crystal. Sc-Si PV cells give slightly higher efficiencies than mc-Si cells but they require two-axis tracking systems since the efficiency drops quickly when the panel is not perpendicular to the radiation. Therefore mc-Si panels are often used instead of sc-Si panels since the efficiency is less affected by the angle of radiation to the panel.

Amorphous silicon (a-Si)

Amorphous silicon has no crystalline structure. The efficiency is low and therefore amorphous silicon has never been popular to be used in PV cells. Amorphous silicon can though be used to produce so called *thin-film* PV cells, which is a flexible film of PV cells.

Cadmium-Telluride (CdTe)

Cadmium telluride is also a material that is used to produce thin-film photovoltaics. It has a significantly higher efficiency than a-Si PV cells and can be compared to the efficiencies that are reached in crystalline silicon PV cells. It is used in the largest solar power plants in the world because of its low production cost and high efficiency.

2.1.3. Photovoltaic characteristics

Volt-ampere characteristics

The V-A- and power characteristics for a photovoltaic can be seen in Figure 2.3. What characterizes a photovoltaic is the open-circuit voltage, U_{OC} and the short-circuit current, I_{SC}. There exists a point where the maximum power can be drawn from the PV. This point is called the *maximum power point* (MPP). In Figure 2.3 this is denoted as point [U_{mpp}; I_{mpp}]. It corresponds to a terminal voltage, U_{mpp} and a current, I_{mpp} where the maximum power is generated.

A factor that defines the quality of the photovoltaic is the *fill factor* (FF). It is defined as the ratio between MPP and the theoretical power, defined from U_{OC} and I_{CS} as follows (3):

$$FF = \frac{U_{mpp} \cdot I_{mpp}}{U_{OC} \cdot I_{SC}} \qquad [\,-\,;\ V,\ A,\ V,\ A] \qquad (2.1)$$

where: U_{mpp} is the terminal voltage at MPP
I_{mpp} is the terminal current at MPP
U_{OC} is the open-circuit voltage
I_{SC} is the short-circuit current

Equation 2.1 is also depicted as the two areas in Figure 2.3. *Area A* corresponds to the maximum power or $U_{mpp} \cdot I_{mpp}$ as denoted in the formula for fill factor. *Area B* corresponds to the theoretical power or $U_{OC} \cdot I_{SC}$. When the fill factor is large, the V-A characteristic of the photovoltaic is more square-like and respectively when the fill factor is small the V-A characteristic is less square-like. The fill factor therefore describes the slope of the V-A characteristic. When designing photovoltaics, a large fill factor is desired since it means a greater power output from the cell. A large fill factor can be obtained when the series resistance R_s is small and the shunt resistance R_{sh} is large in the PV cell. These resistances can be seen in the equivalent circuit for the PV cell in Figure 2.2 on page 18.

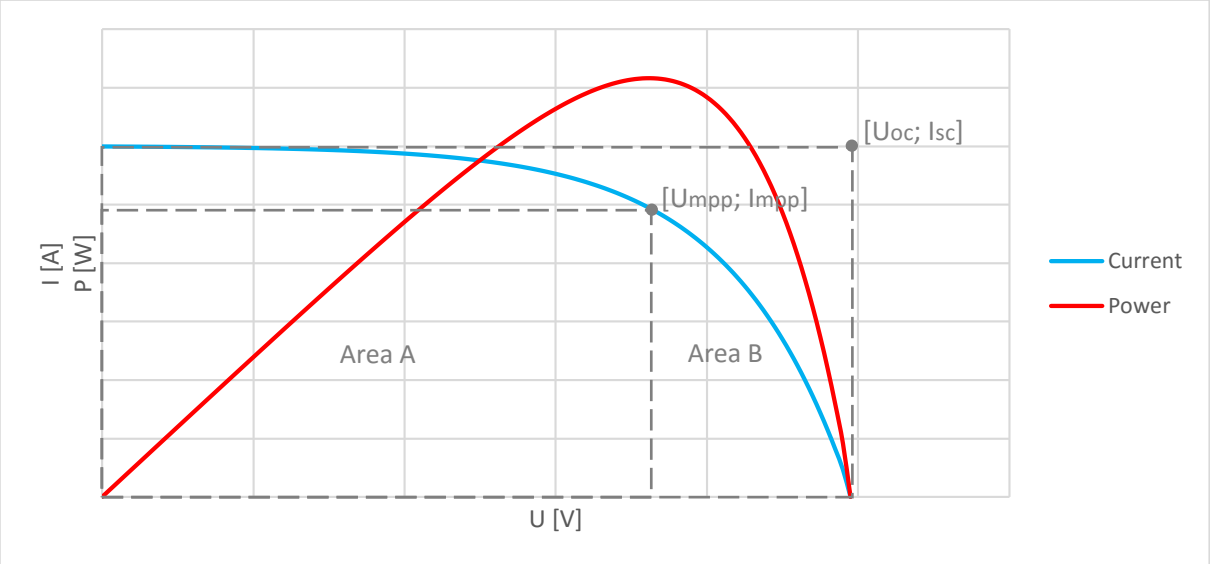

Figure 2.3 – Volt-ampere- and power characteristics of a photovoltaic

The efficiency of a photovoltaic can easily be calculated as a ratio between the maximum power output and the radiated power to the panel. The expression:

$$\eta = \frac{U_{mpp} \cdot I_{mpp}}{E \cdot A} \cdot 100\% \qquad [\,\%\,;\ \mathrm{V},\ \mathrm{A},\ \mathrm{W/m^2},\ \mathrm{m^2}] \qquad (2.2)$$

where: U_{mpp} is the terminal voltage at MPP
I_{mpp} is the terminal current at MPP
E is the perpendicular irradiance
A is the area of the photovoltaic

The theoretical current output from a photovoltaic can be calculated by:

$$I_{cell} = I_{ph} - I_o \cdot \left[exp\left[\frac{e \cdot (U_{cell} + I_{cell} \cdot R_s)}{n \cdot k \cdot T} \right] - 1 \right] - \frac{U_{cell} + I_{cell} \cdot R_s}{R_{sh}} \qquad (2.3)$$

[A; A, A, C, V, A, Ω, -, J/K, K, V, A, Ω, Ω]

where: I_{ph} is the current generated by photons
I_o is the saturated leakage current
e is the electron charge ($1{,}6021773 \cdot 10^{-19}$C)

U_{cell} is the voltage at the photovoltaic terminals
I_{cell} is the current at the photovoltaic terminals
R_s is the series resistance
n is the number of cells connected in series
k is the Boltzmann constant (1,380658·10^{-23}J/K)
T is the absolute temperature
R_{sh} is the shunt resistance

Equation 2.3 can be simplified so that:

$$U_{cell} + I_{cell} \cdot R_s = \Delta U_{sem} \approx U_{cell} \qquad \text{[V, A, Ω; V]} \qquad (2.4)$$

where: ΔU_{sem} is the voltage between the conduction band and the valence band

and

$$\frac{U_{cell} + I_{cell} \cdot R_s}{R_{sh}} = I_{Rsh} \approx 0A \qquad \text{[V, A, Ω, Ω; A]} \qquad (2.5)$$

Equation 2.4 corresponds to the voltage that is inside the cell, between the conduction band and the valence band. In Figure 2.2 it could be understood as the voltage across the current source or the voltage across the shunt resistor, R_{sh}. Since the series resistance, R_s is small, the voltage drop over the resistor is small and it can be assumed that ΔU_{sem} equals to the cell terminal voltage, U_{cell}.

Equation 2.5 on the other hand corresponds to the current, I_{Rsh} through the shunt resistor, R_{sh}. It can be generalized that this current is close to zero since the shunt resistance, R_{sh} is large, and therefore it can be neglected. It is also to be noted that Equation 2.3 can only give an estimation of the photovoltaic current output since the parameters are also functions of both temperature and irradiance.

Temperature and irradiance influences
Temperature and irradiance influences to photovoltaic performance are complicated to calculate since the irradiance affects not only the power output but also the temperature of the PV and temperature on the other hand affects resistances and current generation in the PV.

It can be generalized that a temperature difference influences the V-A characteristic so that it shifts horizontally. A higher temperature decreases the output power and shifts the V-A characteristic to the left and a lower temperature on the other hand increases the power output and shifts the V-A characteristic to the right. A small change can also be seen in the vertical direction where a temperature increase shifts the characteristic slightly upwards and a temperature decrease shifts it slightly downwards. An example of this can be seen in Figure 2.4 on the left. It holds that T1>T2>T3.

Similarly it can be generalized that a difference in irradiance shifts the V-A characteristics vertically. A higher irradiance shifts the V-A characteristic upwards and a lower irradiance shifts the characteristic downwards. This is depicted in Figure 2.4 on the right. It holds that E1<E2<E3.

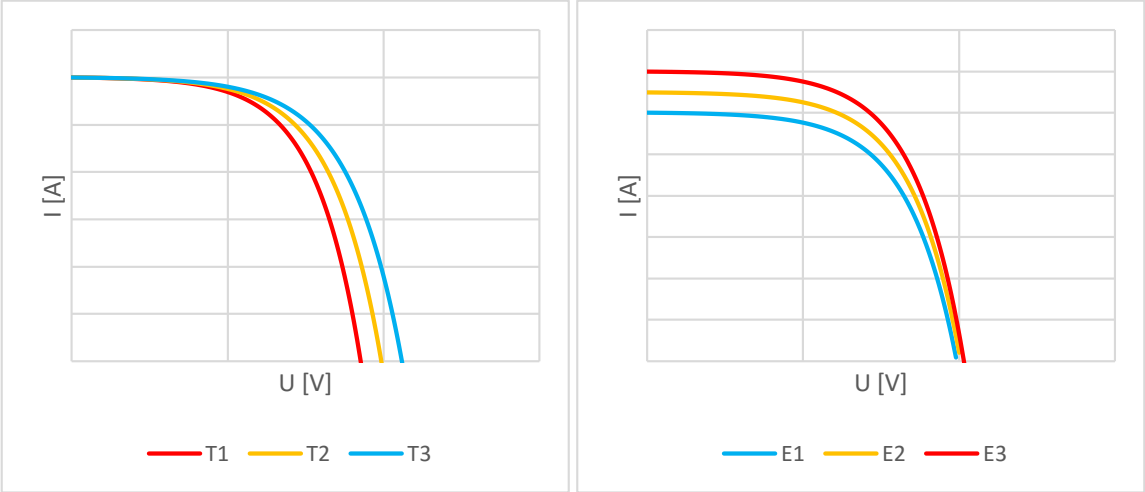

Figure 2.4 – Temperature (left) and irradiance (right) influences on V-A characteristics

2.1.4. Photovoltaic power system

Several external components are needed for a proper operation of PV panels in a power system, either to be connected to the grid or for a local connection. The central component, which is used in both configurations, is the *maximum power point tracker* (MPPT). Other components are rectifiers, inverters, control systems and battery storages.

Maximum power point tracker (MPPT)

The MPP changes location according to the position of the sun during the day or due to passing clouds in front of the PV. Therefore the maximum power that can be drawn from a PV changes. The MPPT is used to track this point for every moment so that the PV operates ideally for different irradiances. The task is to find the voltage and current where the maximum power is produced for every moment. The MPPT often use *pulse width modulation* (PWM) to get the right power output.

The MPPT is often the first part in the PV power system. From the MPPT the current is then fed further to other parts of the system such as a battery storage system or a *power conditioning system*.

Power conditioning system (PCS)

The PCS has a number of functions it has to perform. First it has to monitor the output power from the MPPT and the battery system, which is connected in parallel, and adjust its output power according to the power that is available. It should also convert the DC voltage to an AC voltage by the help of an inverter and monitor the utility system to supply appropriate power.

Other components

A *battery storage* is often used to smooth out rapid power changes from the photovoltaics so that a more stable power is produced. It is also used so that when no power is utilized from the system, the photovoltaics could still produce power and store it in the battery storage so that it could be used later when possibly no power is generated by the photovoltaics.

In grid connections a *power detector* is used to measure the power that is fed to or from the grid. It also checks that the power has appropriate quality and it can turn off the connection to the power grid in case inappropriate power is generated or a fault is detected in the power grid or the local system.

A *control system* controls that all the different parts work ideally together. It controls circuit breakers in the system and monitors what power is available from the photovoltaics and if needed, switches over to the grid connection.

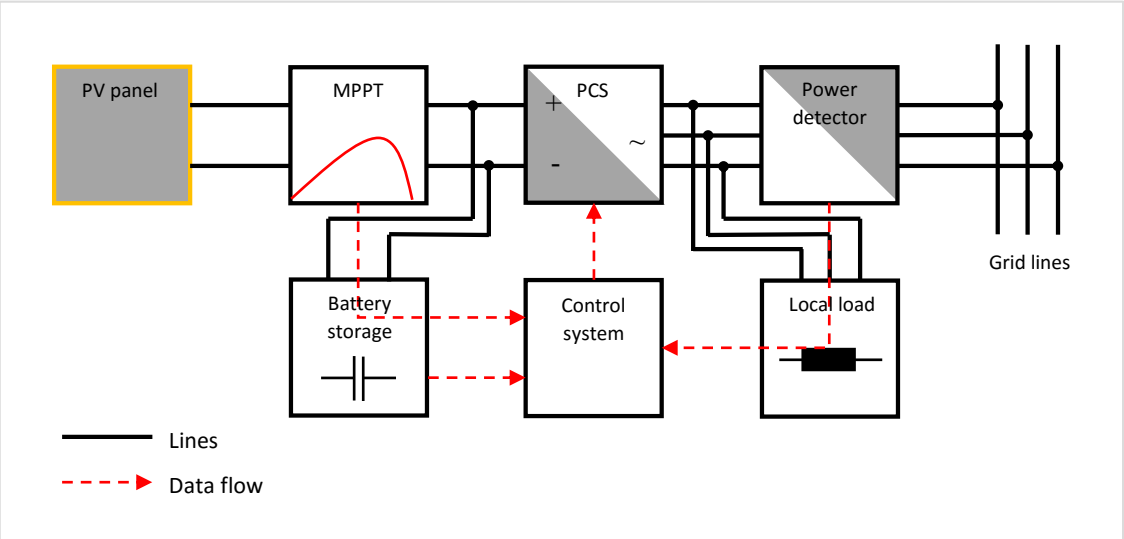

Figure 2.5 – Block diagram of photovoltaic power system connected to the grid

Requirements for connection to the grid

There are several legal and technical requirements that has to be met before a photovoltaic system can be connected to the net. We will discuss the technical aspects according to the standards in Finland.

The central requirement is the standards for the protections that are used. The requirements for protections are divided into two groups according to the size of the generation plant, for plants under 50 kVA and above 50 kVA but up to 10 000 kVA. The basic requirements for both groups are that voltages and frequencies has to stay within certain limits. Protections should disconnect the generation plant within a certain time from the grid in case voltages or frequencies are outside the given limits. The plant should neither work in an idle state where the grid voltage is close to zero.

Before connecting a generation plant such as a photovoltaic system to the grid, it has to be discussed with the grid operator to make sure that the new connection will not disturb the grid (10).

2.2. Concentrated Solar Power (CSP)

CSP systems capture the sunlight by help of mirrors and concentrates it to a heat receiver. There are different designs according to configuration of receivers and mirrors. They can be divided into two main groups, *Line-focusing systems* or *Point-focusing systems* (11). Line-focusing systems use mirrors that have single-axis tracking and the receiver is located on a focal line above the mirrors. Point-tracking systems, on the other hand, use two-axis tracking and the sunlight is concentrated to a single point where the receiver is located.

CSP systems need high irradiance since they can only absorb the direct part of the sun's radiation. Therefore they need to be located at the "Sun belt" where sun radiation is high. This is at locations of 40 degrees north and south of the equator.

The heat that is received by the receiver is absorbed by a *heat transfer fluid* so that the heat can be used in a conventional steam turbine configuration. There are also designs where the heat transfer is

done directly by boiling water in the receiver and the steam is fed directly into the steam turbine. In those designs a possible *heat storage* is harder to design and often becomes more costly. Synthetic oil or molten salt can be used as heat transfer fluid. Molten salt is preferred since it can store more heat and operate with higher temperatures, which on the other hand increases the efficiency.

A heat storage can be used to smooth out fast variations in irradiance or to produce electricity at night or in cloudy conditions. A heat storage increases therefore the *capacity factor* of the system. Molten salt is often preferred before oil in a thermal storage since molten salt has a higher thermal capacity, which reduces the volume needed for storing heat.

CSP systems are often used for cogeneration to not only produce electricity but also heat for space heating or process heat. This is due to the fact that the heat is used in a similar way as in a conventional steam turbine and the water cycle corresponds to the *Rankine cycle*. The heat from the condensing process can be used to produce useful heat. This increases the efficiency of the plant in the same way as it does for a conventional steam turbine configuration.

2.2.1. Line-focusing CSP systems

Parabolic Trough collectors (PTC)

PTC systems consist of long parabolic mirrors and a receiver tube at the focal point of every mirror. The tracking system move the mirrors and the receiver tubes usually from east to west as the sun moves on the sky and the mirrors are aligned in a north-south position. The heat transfer fluid used is often synthetic oil. The heat is transferred to a steam turbine or a thermal storage often consisting of molten salt.

The parabolic mirrors can be up to 100 meters long and have a curved aperture of 5-6 meters. The receiver consist of a metal tube inside a glass envelope to reduce thermal losses. The metal tube is often stainless steel with the heat transfer fluid inside of it. The tube has a coating that absorbs the sunlight spectrum well and emits infrared radiation poorly. This way the maximum heat is absorbed and the minimum heat is lost to the surroundings.

PTC systems account for more than 90 % of all CSP systems that are installed. It is the most mature system used today. The efficiency often lay between 14-16 % (12).

Linear Fresnel collectors (LFC)

The LFC configuration has a fixed receiver several meters above the collector mirrors. The mirrors are flat or slightly curved and they are separately tracked on one axis towards the sun to reflect the sunlight to the receiver. The receiver tube requires a secondary mirror above it to refocus the radiation that misses it because of the distortion due to astigmatism. It is also possible to use several absorber tubes beside each other to widen the area of the receiver to collect the unfocused rays.

The efficiency of LFC is slightly lower than for PTC because of higher optical losses (12).

Figure 2.6 – Parabolic Trough collector (left) and Linear Fresnel collector (right)

2.2.2. Point-focusing CSP systems

Solar Towers (ST)

A ST system comprises of several mirrors or heliostats that are individually tracked to reflect the sunlight to a central receiver on top of a tower. The receiver on top of the tower absorbs the thermal energy to a heat transfer fluid. The heat is then used in a steam generator or it is used for district heating, similarly as in the Line-focusing CSP systems.

Molten salt, oil, water or even gas can be used as a heat transfer fluid in a ST system. Depending on the used fluid, different operation temperatures are derived. The lowest operation temperature is for water steam as heat transfer fluid and gas has the highest operation temperature.

Thermal storages are also used to store thermal energy so that it can be used later when no irradiance is received by the collector mirrors.

In large ST plants the distance between the heliostats and the receiver tower can be large. This increases the losses due to light absorption in the atmosphere and angular deviations also increase due to imperfections in the mirrors and the sun-tracking system (12).

Solar Dishes (SD)

SD technology uses a parabolic mirror or collector and a receiver in the focal point of the parabolic mirror. The big mirror use two-axis tracking to always be pointed towards the sun. The receiver can be a Stirling engine that use the difference in air temperature to move a piston. The receiver can also be a micro-turbine. Lot of research is done to optimize Stirling engines to be used in SD systems.

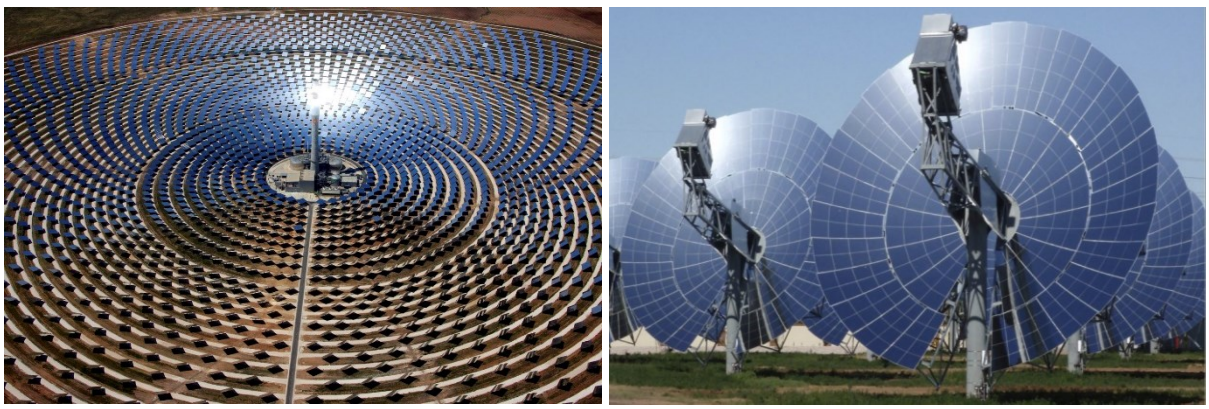

Figure 2.7 – Solar Tower plant (left) and Solar Dishes (right)

2.3. NATURE OF SUNLIGHT

2.3.1. Irradiance

Above the earth's atmosphere the radiation intensity or irradiance from the sun is considered to be at a constant value of 1 353 W/m^2. On the surface of the earth with a clear sky the irradiance is smaller, often considered to be at 1 000 W/m^2 (13). The irradiance on the surface of the earth is smaller because of the absorption, scattering and reflection in the atmosphere. The light that is scattered or reflected either from the atmosphere or from objects around a PV panel is referred to *as indirect irradiance* to the PV panel. *Direct irradiance* is the radiation directly from the sun to the PV panel. When clouds pass in front of the sun, the direct irradiance decreases strongly while the indirect irradiance increases somewhat. The small increase is due to the fact that scattering and reflection of the radiation from the sun increases in a cloud.

The atmosphere also absorbs the radiation differently depending on the position of the sun on the sky. The irradiance decrease fast when the sun goes below 10 degrees from the horizon.

2.3.2. Sunlight spectrum

The spectrum of sunlight is also different above the atmosphere and on the surface of the earth. This is due to the fact that some wavelengths of the radiated sunlight are absorbed, scattered and reflected in the atmosphere in a greater scale than others. Therefore the intensity of some wavelengths are smaller than others. The spectrum of sunlight is measured in *Air mass*. Above the atmosphere the spectrum is referred to as the *Air mass zero* (AM0) spectrum, while on the surface of the earth, when the sun zenith angle is 0°, the air mass coefficient is 1 (AM1). In photovoltaic measurements the air mass coefficient is considered to be 1,5 (AM1,5). The value of the air mass coefficient is dependent on the elevation angle (or the zenith angle) of the sun, as described in Chapter 2.3.3. The lower the sun is on the sky, the higher is the air mass coefficient. This is due to the fact that sunlight need to travel a longer distance through the atmosphere when the elevation angle is smaller and therefore a greater amount of the light is absorbed, scattered and reflected on its way through the atmosphere.

2.3.3. Position of the sun

The movement and position of the sun can be predicted with a high accuracy for a long timescale beforehand for different locations. Thus the power generation of a PV panel can also be estimated accurately. The position of the sun and the direction and tilt of the PV panel are the main factors that affect the generated power. The position of the sun can be calculated by help of the *celestial coordinates* and more specifically the *declination*, which is used to indicate the position of stars and planets on the sky. The declination for the sun is defined as (14):

$$\delta = 0{,}4093 \cdot \cos\left(2\pi \cdot \frac{d - 173}{365}\right) \qquad \text{[rad; -]} \qquad (2.6)$$

where: d is the number of the day of the year

To "translate" the declination into horizontal coordinates we need to define the *hour angle*. The hour angle defines the position of the sun to a specific location at a specific local time. It is defined as (14):

$$\omega = 2\pi \cdot \frac{T_{UC}}{24} - \lambda_e \qquad \text{[rad; h, rad]} \qquad (2.7)$$

where: T_{UC} is the coordinated local time
λ_e is the longitude of the location

When the declination and hour angle are known, we can calculate the horizontal position of the sun defined as *elevation,* ψ_s and *azimuth,* A_s. The elevation is defined as the angle between the sun and the horizon. The azimuth on the other hand is defined as the angle between the sun and the geographical North Pole. The angles are also depicted in Figure 2.11 on page 30. The expressions for elevation and azimuth are as follows (14):

$$\psi_s = \sin^{-1}(\sin\phi \cdot \sin\delta - \cos\phi \cdot \cos\delta \cdot \cos\omega) \quad \text{[rad]} \quad (2.8)$$

where: ϕ is the latitude of the location
δ is the declination
ω is the hour angle

$$A_s = \cos^{-1}\left(\frac{\cos\phi \cdot \sin\delta - \sin\phi \cdot \cos\delta \cdot \cos\omega}{\cos\psi_s}\right) \quad \text{[rad]} \quad (2.9)$$

where: ϕ is the latitude of the location
δ is the declination
ω is the hour angle
ψ_s is the elevation angle for the sun

As already mentioned, solar power is not an ideal power source in Finland. This can easily be seen in Figure 2.8 where the elevation and azimuth of the sun is plotted of the lightest day of the year and respectively the darkest day in Helsinki, located in the most south of Finland. In June the irradiance is acceptable to produce electricity with a PV panel but during winter time almost no power is generated since the sun is so low on the sky. This is due to the fact that the irradiance from the sun decreases drastically when the sun elevation is below 10 degrees, as already mentioned. From the figure it is seen that in Helsinki the sun will not reach that elevation during the darkest time and this time-period is about two months (15).

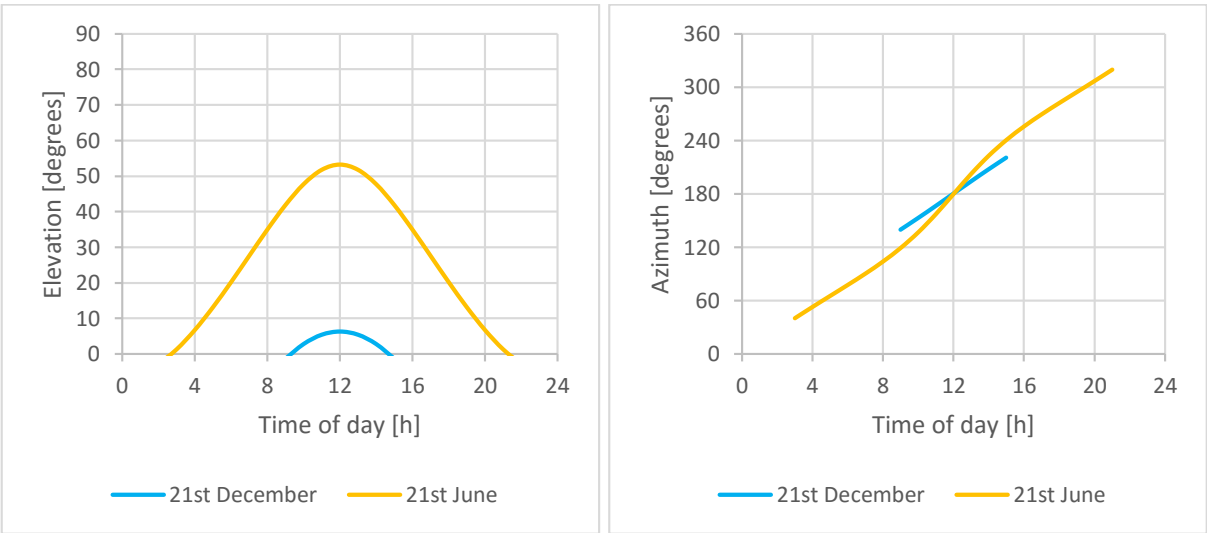

Figure 2.8 – Elevation and azimuth in Helsinki, Finland (60°N)

The profitability of solar power decreases fast when going north in Finland. The elevation and azimuth in Rovaniemi, located at the Arctic Circle is seen in Figure 2.9. As seen, the sun just reaches the horizon during the darkest time but stays otherwise under the horizon. During the lightest time in summer, the sun will not go down at all. The time-period when the sun will not reach higher than 10 degrees above the horizon is about four months here (15). The elevation angle during the lightest period is not much lower in Rovaniemi than it is in Helsinki. Since the elevation angles does not differ that much during summer time between Helsinki and Rovaniemi but greater in winter time, the fluctuation in irradiance is greater in Rovaniemi and therefore also the expected generated power fluctuates more between seasons.

Figure 2.10 shows the elevation and azimuth in Prague, Czech Republic. Even in wintertime the sun always reaches above 10 degrees of the horizon. During summer the maximum elevation is about 10 degrees more than in Helsinki and almost 20 degrees more than in Rovaniemi. This makes it possible to produce electricity with photovoltaics throughout the whole year and in summer the irradiance is relatively large.

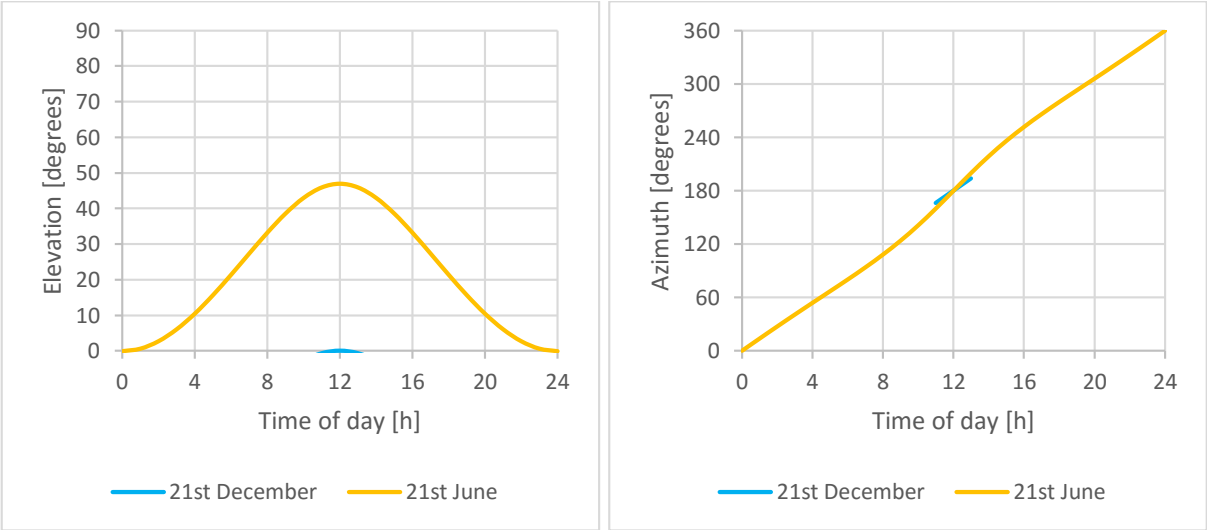

Figure 2.9 – Elevation and azimuth in Rovaniemi, Finland (66°N)

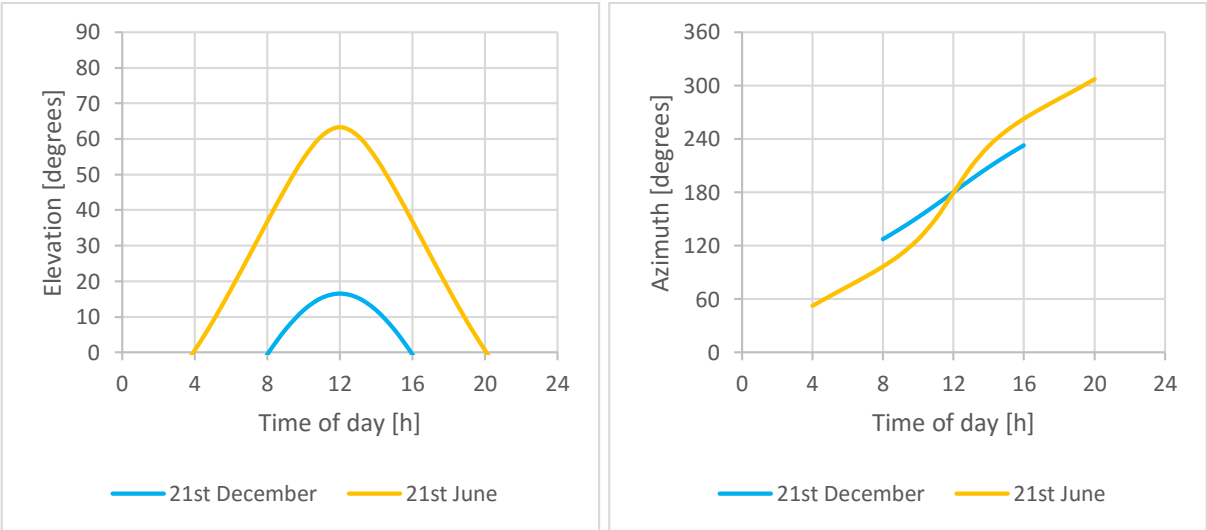

Figure 2.10 – Elevation and azimuth in Prague, Czech Republic (50°N)

2.3.4. PV panel tilt

By tilting a PV panel so that it is perpendicular to the radiation results in that more sunlight is absorbed by the panel and more power is produced. In an ideal configuration the PV panel moves during the day to always be facing the sun. This way the angle between the radiation and the perpendicular of the panel is minimized for every time of the day. It is expensive to design such a system and therefore they are only used in large scale photovoltaic plants.

In general the tilt of a stationary PV panel should be approximately the same as the latitude of the location. With this configuration the maximum amount of power will be produced throughout the year.

The angle between the sun and the perpendicular of a PV panel can be calculated using the following expression (14):

$$\alpha = \cos^{-1}\left(\sin\psi_p \cdot \sin\psi_s + \cos\psi_p \cdot \cos\psi_s \cdot \cos\left(A_s - A_p\right)\right) \quad \text{[rad]} \quad (2.10)$$

where: ψ_p is the elevation angle of the PV panel
ψ_s is the elevation of the sun
A_p is the azimuth of the PV panel
A_s is the azimuth of the sun

The angle is also depicted in Figure 2.11. Further the estimated irradiance to the panel with no cloud cover can be expressed as (14):

$$E = \cos\alpha \cdot (-24{,}1 + 894{,}8 \cdot \sin\psi_s + 238{,}4 \cdot \sin^3\psi_s) \quad \text{[W/m}^2\text{; rad, rad, rad]} \quad (2.11)$$

where: α is the angle between the sun and the perpendicular of the PV panel
ψ_s is the elevation of the sun

The different components of the sun elevation is due to the fact that the irradiance from the sun also depends on the elevation of the sun. Under an elevation of 10 degrees the irradiance is small but around 10 degrees it increases drastically and stays relatively constant above that.

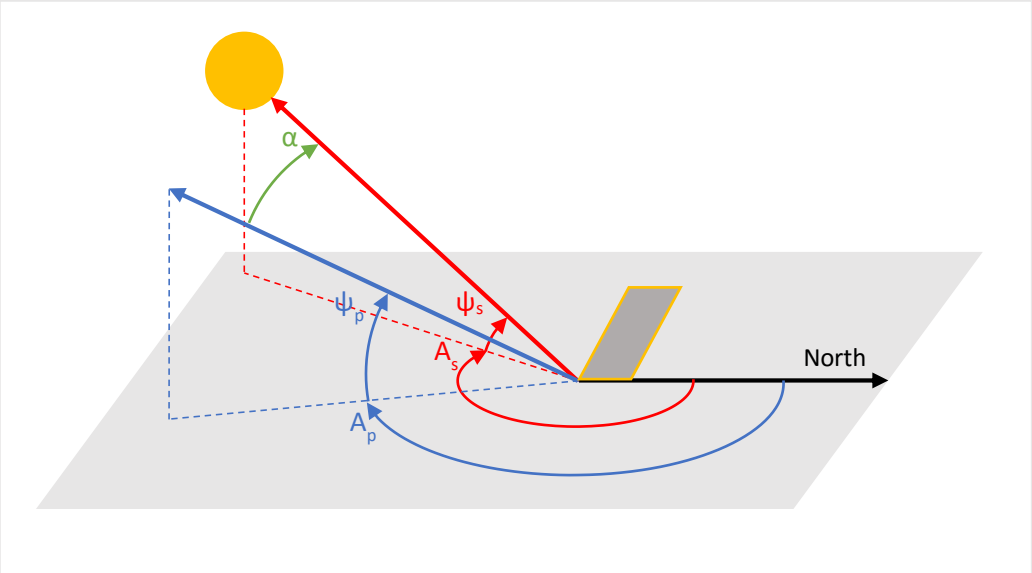

Figure 2.11 – Elevation and azimuth angles of the sun and a PV panel

2.3.5. Cloud coverage

Clouds are the main cause for fast and great variations in produced power from a PV panel. Cloud coverage is hard to estimate even hours beforehand and it is the main cause for making photovoltaics an unpredictable source of energy.

Cloud coverage is measured in *oktas*. Zero okta corresponds to a totally clear sky and 8 okta means a fully clouded sky. A 5 okta cloud coverage means that 5/8 of the sky is covered by clouds. The thicker the cloud coverage is, the less radiation is received to the surface of the earth. It is estimated that for a fully clouded sky less than 25 % of the radiation above the atmosphere reaches the earth, when for a fully clear sky the number is 80 % (16).

3. MEASUREMENT OF PHOTOVOLTAICS

This chapter covers the practical measurements of photovoltaics. In Chapter 3.1 we measure the characteristics of two PV cells of model SM330, which are used for educational purposes. We calculate the ideal size of the load resistor that is used while measuring the V-A characteristics of the cells. Light spectrum influences are also measured for the cells.

Further, in Chapter 3.2, we compare a mono- and a polycrystalline photovoltaic.

3.1. TWO PHOTOVOLTAIC CELLS SM330

The aim of this measurement is to clarify the theories and the approach for measuring for two photovoltaic cells of model SM330 (0,5 V / 330 mA) as seen in Figure 3.1, which are used for educational purposes. Measurements include volt-ampere characteristics for different inclinations of the cells, light spectrum influences and calculation of efficiency and fill factor. Measurements are made for both a series- and a parallel connection. A laboratory measurement that can be used by students is enclosed in Appendix VIII on page 59.

The goal is also to specify the best size for the load resistor that is used during the measurement of the cells, so that resistors of the right size could be procured. That topic is covered in Chapter 3.1.3.

Figure 3.1 – Two photovoltaic cells, Monocrystalline SM330, 0,5V/330mA

3.1.1. PV cell characteristics and inclination influences

The setup

The volt-ampere characteristics were measured for both a series- and a parallel connection of the two cells for different inclinations. The measurement was made in a dark room to decrease the indirect radiation to the cells. An incandescent, 60 W lamp was placed 25 cm from the cells and the irradiance was measured to be approximately 12,5 W/m^2 on the surface of the cells. The dimensions of one cell was measured to be 52 mm x 21 mm.

Totally ten cases were measured with inclination angles of 0°, 20°, 40°, 60° and 80° for both a series- and a parallel connection of the cells. The inclination angle is defined as the angle between the direction of the radiation and the perpendicular of the cells. The radiation was constant throughout the whole measurement. The temperature at the cells increased during the measurement by 3 °C due to the heat from the incandescent lamp. A list of used apparatus and a connection diagram of the measurement can be seen below:

Solar cell x2, Monocrystalline SM330 0,5 V / 330 mA
Incandescent lamp, 60 W
Multimeter x2, Voltcraft VC155
Irradiance and temperature meter, PRC Krochmann RadioLux 111
Variable resistor, 39 Ω / 4 A
Variable resistor, 570 Ω / 1 A

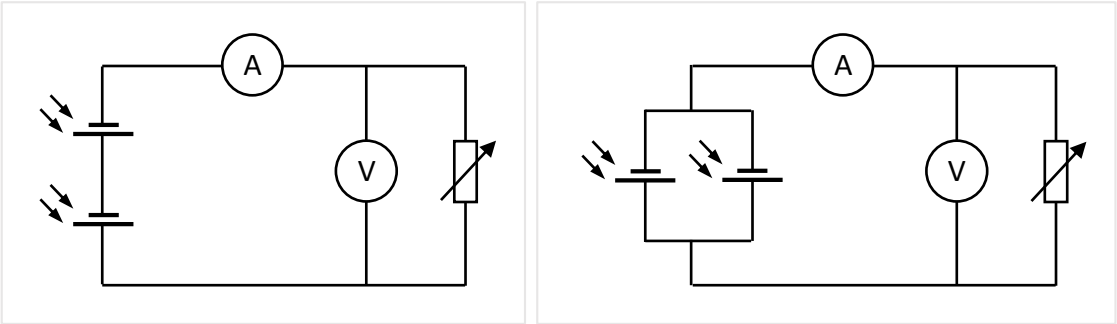

Figure 3.2 – Series connection (left) and parallel connection (right) of V-A characteristics measurement with two solar cells SM330

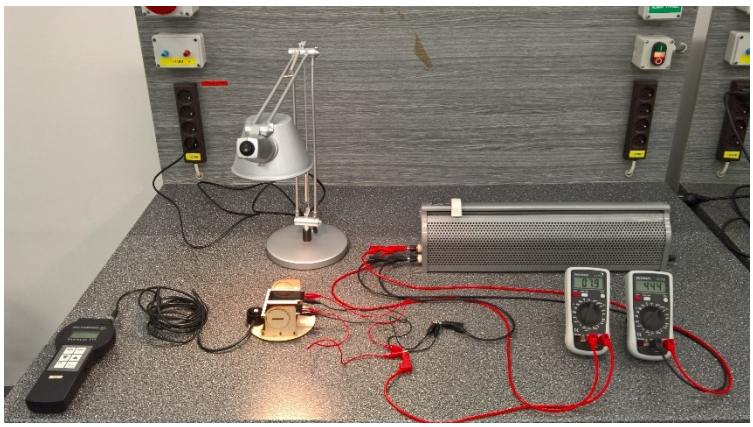

Figure 3.3 – Setup of V-A characteristics measurement with two solar cells SM330

Results

The volt-ampere characteristics were measured for every inclination of the cells for both a series- and a parallel connection. The results can be found in Appendix I on page 49 for the series connection and the results for the parallel connection can be found in Appendix II on page 50. The generated power was calculated simply by multiplying the measured current and voltage:

$$P = U \cdot I = 0{,}5V \cdot (1{,}586 \cdot 10^{-2})A = (7{,}93 \cdot 10^{-3})W \rightarrow 7{,}93mW \quad (3.1)$$

The example values that are used in the above equation are coloured in Appendix I. The volt-ampere and power characteristics are plotted for both the series- and the parallel connection:

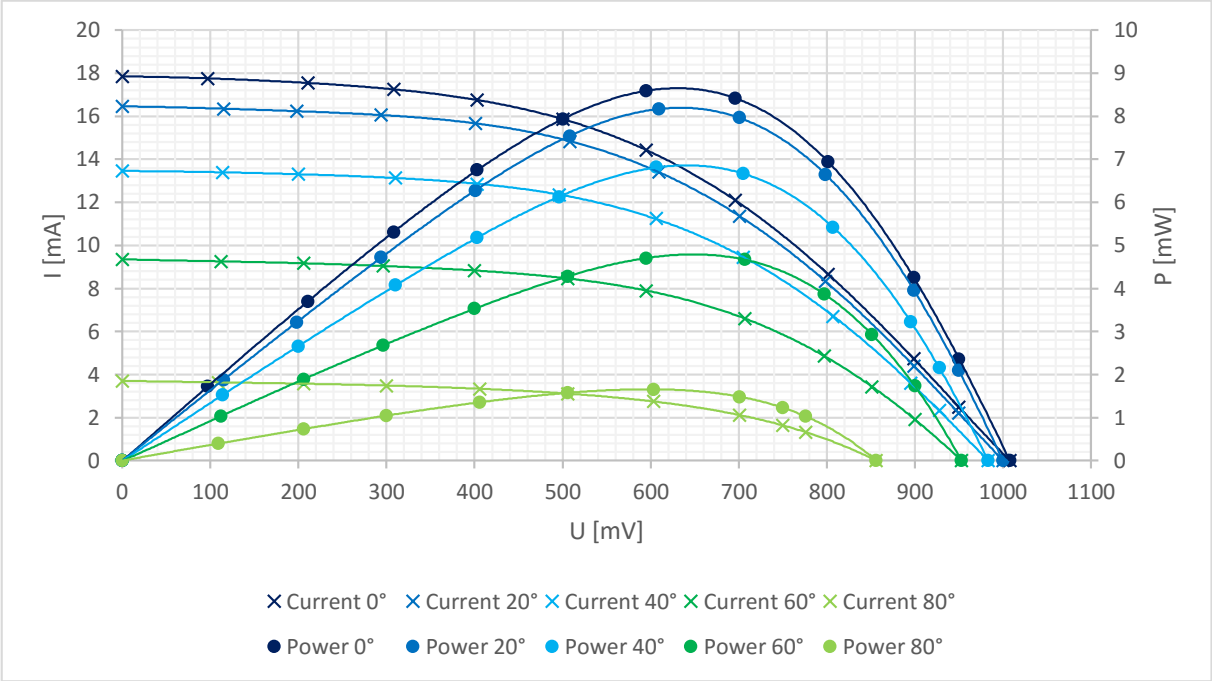

Figure 3.4 – Plot of V-A and power characteristics of series connection of two solar cells SM330 for different inclinations

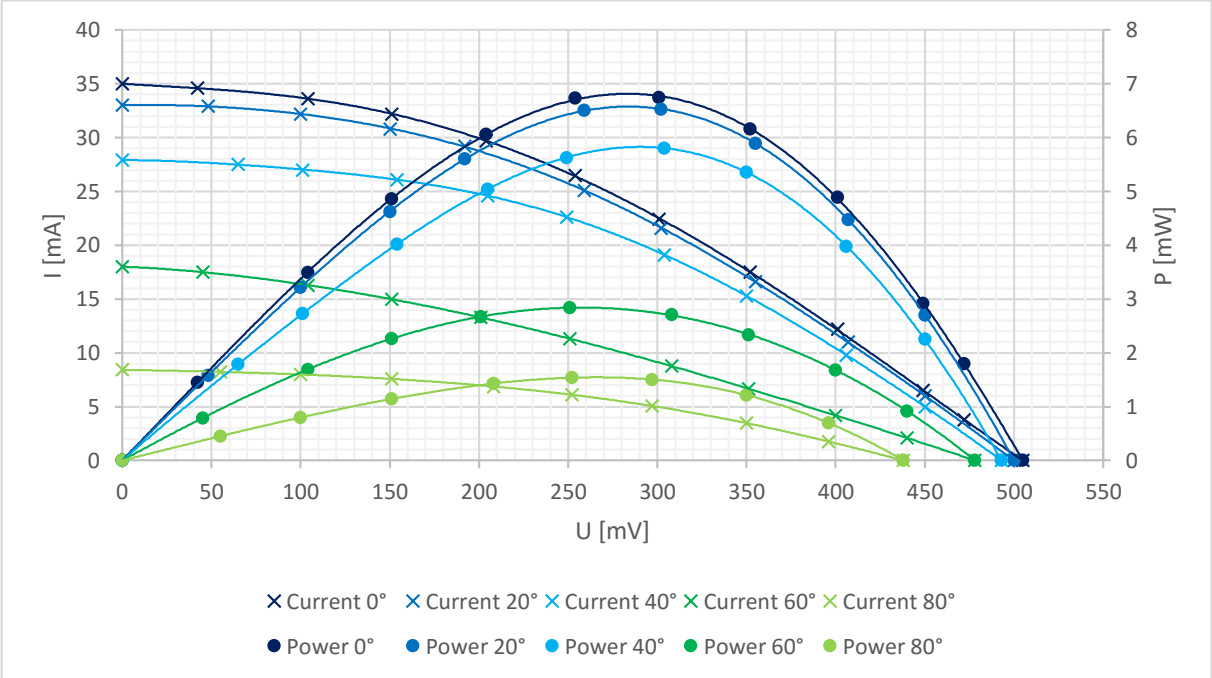

Figure 3.5 – Plot of V-A- and power characteristics of parallel connection of two solar cells SM330 for different inclinations

We can graphically find the power at MPP, P_{mpp} for both the series- and the parallel connections from Figure 3.4 and Figure 3.5. For the series connection and for an inclination of 0° the power is P_{mpp} = 8,65 mW. For the parallel connection P_{mpp} = 6,80 mW, also for an inclination of 0°. From the measured values we can also find the open circuit voltage, U_{OC} and short circuit current, I_{SC}. For the

series connection U_{OC} = 1008 mV and I_{SC} = 17,85 mA. For the parallel connection on the other hand U_{OC} = 505 mV and I_{SC} = 35,0 mA.

With these data known, we can calculate the fill factor for an inclination of 0° for both the series- and the parallel connections. For the series connection it holds:

$$FF_s = \frac{U_{mpp} \cdot I_{mpp}}{U_{OC} \cdot I_{SC}} = \frac{P_{mpp}}{U_{OC} \cdot I_{SC}} = \frac{(8{,}65 \cdot 10^{-3})W}{1{,}008V \cdot 0{,}01785A} = 0{,}481 \tag{3.2}$$

For the parallel connection it holds:

$$FF_p = \frac{U_{mpp} \cdot I_{mpp}}{U_{OC} \cdot I_{SC}} = \frac{P_{mpp}}{U_{OC} \cdot I_{SC}} = \frac{(6{,}80 \cdot 10^{-3})W}{0{,}505V \cdot 0{,}035A} = 0{,}385 \tag{3.3}$$

Measured efficiency can be calculated by using Equation 2.2 on page 20. We start with calculating the total area of the cells:

$$A = 0{,}052m \cdot 0{,}021m \cdot 2 = (2{,}18 \cdot 10^{-3})m^2 \tag{3.4}$$

Efficiency for the series connection of the cells is calculated:

$$\eta_s = \frac{U_{mpp} \cdot I_{mpp}}{E \cdot A} \cdot 100\% = \frac{P_{mpp}}{E \cdot A} \cdot 100\% = \frac{(8{,}65 \cdot 10^{-3})W}{12{,}5W \cdot m^{-2} \cdot (2{,}18 \cdot 10^{-3})m^2} \cdot 100\% = 31{,}7\% \tag{3.5}$$

Efficiency for the parallel connection of the cells is calculated:

$$\eta_p = \frac{U_{mpp} \cdot I_{mpp}}{E \cdot A} \cdot 100\% = \frac{P_{mpp}}{E \cdot A} \cdot 100\% = \frac{(6{,}80 \cdot 10^{-3})W}{12{,}5W \cdot m^{-2} \cdot (2{,}18 \cdot 10^{-3})m^2} \cdot 100\% = 25{,}0\% \tag{3.6}$$

The theoretical efficiency can be calculated from the technical data of the cells. One cell is rated $U_{mpp,t}$ = 0,5 V and $I_{mpp,t}$ = 330 mA when the irradiance to the cell is considered to be at E_t = 1 000 W/m^2. Theoretical efficiency is calculated for one cell only:

$$\eta_t = \frac{U_{mpp,t} \cdot I_{mpp,t}}{E_t \cdot A} \cdot 100\% = \frac{0{,}5V \cdot 0{,}33A}{1000W \cdot m^{-2} \cdot (1{,}09 \cdot 10^{-3})m^2} \cdot 100\% = 15{,}1\% \tag{3.7}$$

Conclusion

It is seen from Figure 3.4 and Figure 3.5 that there is a significant difference in the V-A characteristics between a series connection and a parallel connection of the cells. Obviously the open circuit voltage and the short circuit current differ, but also the shape of the characteristics differ. A series connection of the cells gives a higher power output. The series connection also has a higher fill factor, which means that the cells together have a higher quality than if they would be connected in parallel. In case of a measurement for students, a series connection between the cells would be preferred since the typical V-A characteristic of a photovoltaic is more obvious in that case.

From the plotted results it can also be seen how the inclination of the cells affects the power output. An inclination of 20° does not decrease the power generation much but an inclination greater than that decreases the power output remarkably. In Figure 3.5 a possible error can be seen for the characteristic that is measured for an inclination of 60°. The V-A characteristic line does not follow the trend of the other V-A lines as it has a greater slope on the right side of the MPP.

The calculations for efficiency gave far too high results compared with the theoretical value. The reason for this is most likely an error in the irradiance measurement. It was noted during the measurement that the measured irradiance was greatly affected by the distance to the light source. A change in distance of 1 cm gave a difference of about 5 W/m^2 in irradiance. Further, a small change in irradiance in the calculations of efficiency, affect the result significantly.

As expected the series connection of the cells gave a higher efficiency than the parallel connection since the power output is larger for the series connection as seen in Figure 3.4 and Figure 3.5.

It was also observed during the measurement that the temperature impact to the cells is significant. When a 150 W incandescent lamp was placed close to the cells the short circuit voltage dropped by one third in 10 minutes. It is therefore recommended to measure from a distance. If a 60 W incandescent lamp is used at a distance of 25 cm the temperature increase was measured to be 3 °C. That was the case for this measurement.

It was also noticed that it is possible that a current is induced in the clip wires, which are connected to the cells. It is good to keep this in mind when measuring the V-A characteristics and not to roll up the wires to spools.

3.1.2. Light spectrum influences

The setup

The measurement was started with measuring the spectrum of different lamps in a dark room. Totally six cases were measured for different incandescent lamps, LED lamps and fluorescent lamps. Later the V-A characteristics of the cells were measured for the same lamps and from the same distance between the lamps and the PV cells. A list of used apparatus can be seen below:

Solar cell x2, Monocrystalline SM330 0,5 V / 330 mA
Incandescent lamp, 60 W
Incandescent lamp, 150 W
LED lamp, PILA, 9,5 W
LED lamp, PHILIPS Fortimo LED DLM module 3000, 45 W
Compact fluorescent lamp, PHILIPS Genie, 11 W
Multimeter x2, Voltcraft VC155
Irradiance and temperature meter, PRC Krochmann RadioLux 111
Spectral irradiance colorimeter, EVERFINE SPIC-200BW
Variable resistor, 39 Ω / 4 A
Variable resistor, 570 Ω / 1 A
Variable resistor, 10 000 Ω / 0,25 A

A series connection of the cells was used as seen in Figure 3.2 on the left. A series connection was chosen so that maximal possible power would be generated as we found out in the measurement in

Chapter 3.1.1. The measurement setup was similar as shown in Figure 3.3 on page 32. The only difference was that we measured for different lamps and kept the cells perpendicular to the radiation throughout the measurement.

Results

The results from the spectrum measurement are shown below for the different light sources:

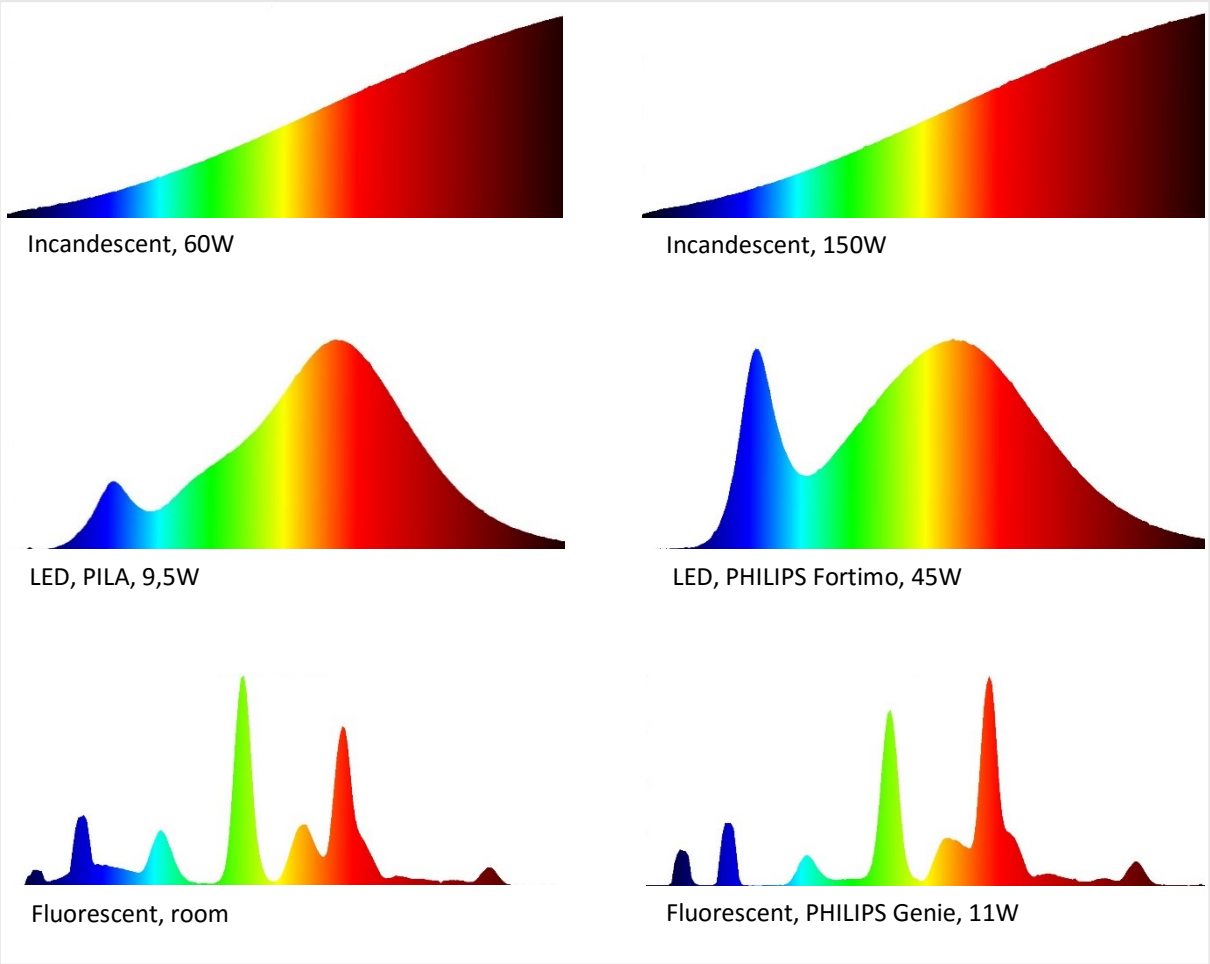

Figure 3.6 – Relative spectrum of different light sources

For every measurement the irradiance was also noted. The results:

Lamp	**Irradiance [W/m^2]**
Incandescent, 60 W	12,44
Incandescent, 150 W	35,97
LED, PILA, 9,5 W	6,21
LED, PHILIPS Fortimo, 45 W	132,11
Fluorescent, room	3,14
Fluorescent, PHILIPS Genie, 11 W	4,44

Table 3.1 – Irradiance from different lamps

For every case, the V-A characteristics of the cells were measured. The measured values can be found in Appendix III on page 51. The output power is calculated by simply multiplying the voltage and the current:

$$P = U \cdot I = 0{,}308V \cdot 0{,}01834A = (5{,}65 \cdot 10^{-3})W \rightarrow 5{,}65mW \tag{3.8}$$

The above values in the example are coloured in the appendix.

Further, a relative value for the power is calculated so that it would be possible to compare the different light sources since they produced different irradiances. This is done by dividing the absolute output power by the irradiance for the specific light source multiplied by the area of the cells. The following values in the example are coloured in the appendix:

$$P_{rel} = \frac{P}{E \cdot A} = \frac{(5{,}65 \cdot 10^{-3})W}{12{,}44W \cdot m^{-2} \cdot (2{,}18 \cdot 10^{-3})m^2} = 0{,}208 \tag{3.9}$$

The area of the cells is calculated in Equation 3.4. After calculating the relative power values for every case, it is noted that the highest value is $P_{relmax} = 0{,}343$. All other values are compared to this maximal value so that a relative percentage can be calculated for the power for all cases:

$$P_{\%} = \frac{P_{rel}}{P_{relmax}} = \frac{0{,}208}{0{,}343} \cdot 100\% = 60{,}65\% \tag{3.10}$$

A relative value for the voltage is also calculated separately for every case. The following values in the example are coloured in the appendix:

$$U_{\%} = \frac{U}{U_{max}} \cdot 100\% = \frac{0{,}308V}{1{,}027V} \cdot 100\% = 29{,}99\% \tag{3.11}$$

The plot of the results:

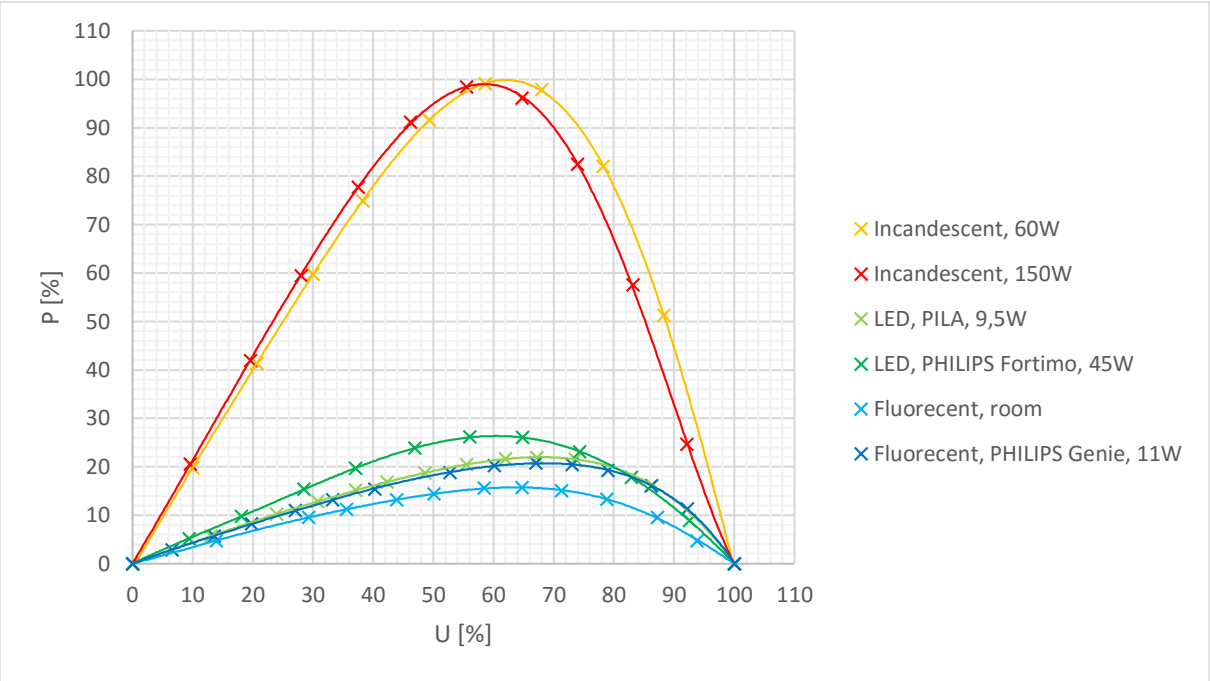

Figure 3.7 – Light spectrum influences to photovoltaic SM330

Conclusion

It can be seen from Figure 3.6 that the incandescent lamps have, as expected, a continuous spectrum corresponding to the spectrum of sun light. The LED lamps have two peaks due to the phosphor coating that converts the short wavelengths of blue light to longer wavelengths of red light. In the spectrum of the fluorescent lamps we see several peaks at different wavelengths. The peaks are produced by the type of the inner coating that is used in the fluorescent tube. We can make the conclusion from the peaks that for example mercury, terbium and europium is used in the coating of both the fluorescent lamps, which we measured (17).

From the plot of the results, in Figure 3.7, it is clearly seen such a great influence the spectrum of the light has on the power generation on the PV cells. The incandescent lamps let the PV cells produce a power about five times larger than with the other lamps. It is seen that the power characteristic of the 150W incandescent lamp is slightly shifted to the left. This is most likely because of the temperature influence from the lamp as described on page 21. It can also be seen that the LED lamps make the PV cells generate a higher power than the fluorescent lamps. The Philips Fortimo LED lamp generates a slightly higher power output than the Pila LED lamp. This might also be possible to ensure by looking at the light spectrum of the LED lamps. The Philips Fortimo LED lamp has a more spread spectrum with more of different wavelengths, while the Pila LED lamp has a narrower spectrum with most wavelengths being around 630 nm. A small difference can also be seen in the power output between the fluorescent lamps. The Philips Genie lamp gives a higher power output at the PV cell terminals than the fluorescent lamps in the measurement room. This can be explained by the fact that the PV cells are most likely designed to absorb long wavelengths better than short ones since sun light has significantly more of long wavelengths than short ones. The light from the Philips Genie lamp has more of long wavelengths than the light from the fluorescent lamps in the room. Therefore the PV

cells are able to absorb more wavelengths from the Philips Genie lamp than from the fluorescent lamps in the room.

3.1.3. Calculation of load resistor size

The setup

The resistor size was calculated for the values that were measured in Chapter 3.1.1. The calculations were made for both the series and the parallel connections as seen in Figure 3.2 but only for a 0° inclination between the cell perpendicular and the radiation. The setup is identical to the one in Chapter 3.1.1 and the same apparatus was used.

Results

The measured and calculated values can be found in Appendix IV on page 53. The power is calculated as in the example Equation 3.1. The resistance is calculated simply by dividing the voltage by the current:

$$R = \frac{U}{I} = \frac{0{,}5V}{0{,}01586A} = 31{,}53\Omega \tag{3.12}$$

The results are plotted:

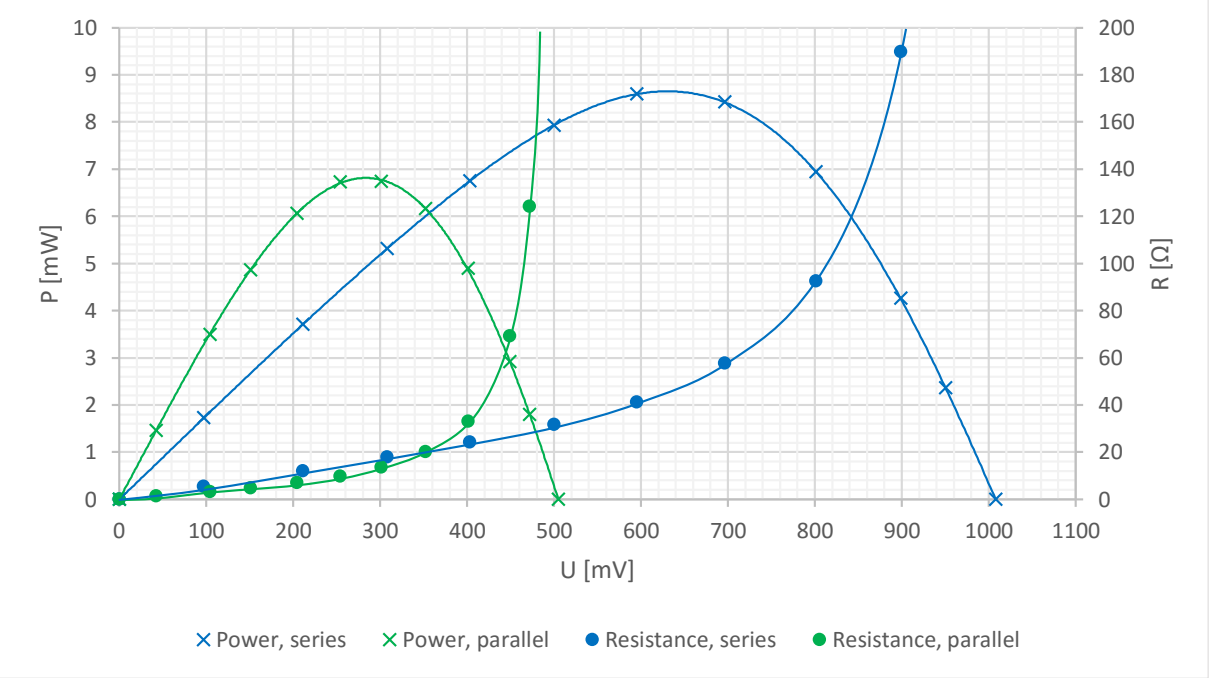

Figure 3.8 – Resistance compared to power output from solar cells SM330

The plot of the results can be found in an enlarged version for better readability in Appendix V on page 54.

Conclusion

It is found from the above figure or Appendix V that in our measurement it is necessary to have a load resistance of at least 46 Ω to be able to measure at MPP for a series connection. For a parallel connection of the cells a 12 Ω load resistance is enough. Tangent lines of the resistance curves can be drawn, as in the appendix. The intersection of the tangent lines correspond to the resistance at MPP.

The required size of the resistor depends on the power output from the cells and therefore also on the irradiance to the cells. A lower irradiance requires a higher resistance while a higher irradiance requires a lower resistance. On the other hand, a series connection requires a higher resistance than a parallel connection.

To be able to measure past MPP the resistance has to be higher than the resistance at MPP. In our measurement a 100 Ω resistance could be used. This allows us to measure past MPP and still the range of the resistor is not too large so that it becomes difficult to measure on the left side of MPP.

The highest current that was measured during all the measurements was 52,70 mA for a series connection of the cells. It was measured for the 150 W incandescent lamp in Chapter 3.1.2. The tolerance of the resistor should be chosen so that it is higher than the highest current that is generated by the cells. A tolerance of for example 100 mA would be enough for a series connection but for a parallel connection, a minimum tolerance of $2 \cdot 52{,}70\text{mA} = 105{,}4\text{mA}$ have to be used.

3.2. Comparison of Mono- and Polycrystalline Photovoltaics

In this chapter we will measure the V-A characteristics for two photovoltaic panels, a monocrystalline of model Siemens T10 and a polycrystalline of model Scott Poly 165. A comparison will be made between the panels regarding inclination influences and power output. The goal is to specify possible differences between the power generation of a monocrystalline and a polycrystalline photovoltaic.

3.2.1. PV panel characteristics and inclination influences

The setup

The monocrystalline PV panel was measured first. The dimensions of the panel were measured to be 31 cm x 63 cm and the irradiance to the panel was $E_{mono} = 7{,}7\ W/m^2$. Several lamps were used to irradiate the panel. The panel was placed so that it was easy to incline it in the direction of the radiation.

The dimensions of the polycrystalline panel were measured to be 153 cm x 76 cm. The irradiance to the panel was $E_{poly} = 2{,}7\ W/m^2$. The panel was placed on the floor since its big size. Several lamps were used to irradiate it.

The V-A characteristics were measured for both the panels for different inclination angles. Inclination angles of 0°, 20°, 40°, 60° and 80° were measured. The inclination of the panels was done so that the panel turned at the middle, so that half of the panel was closer to the lamps and the other half was further away at an inclination. The measurements were made in a dark room so that the irradiance from the lamps in the room would not affect the results. A connection diagram can be seen below for both the measurements and a list of used apparatus during the measurements.

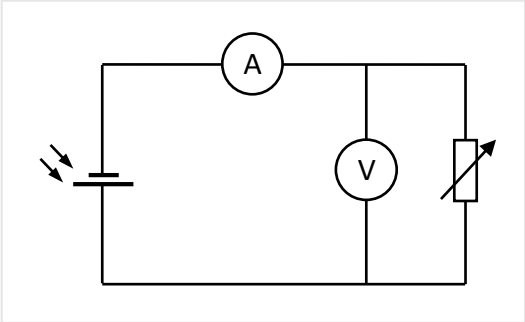

Figure 3.9 – Connection diagram of V-A characteristics measurement of PV panels Siemens T10 and Schott Poly 165

Used apparatus:

PV panel, SIEMENS T10
- U_{mpp} = 16,5 V
- I_{mpp} = 0,61 A
- P_{mpp} = 10 W
- U_{OC} = 23,4 V

PV panel, SCHOTT POLY 165
- U_{mpp} = 35,1 V
- I_{mpp} = 4,7 A
- P_{mpp} = 165 W
- U_{OC} = 43,6 V
- I_{SC} = 5,27 A

Incandescent lamp x2, 60 W
Incandescent lamp, 150 W
LED lamp, PHILIPS Fortimo LED DLM module 3000, 45 W
Multimeter x2, Voltcraft VC155
Irradiance and temperature meter, PRC Krochmann RadioLux 111
Variable resistor, 10 000 Ω / 0,25 A

Figure 3.10 – Measurement setup of Monocrystalline panel Siemens T10 (left) and polycrystalline panel Schott Poly 165 (right)

Results

The voltage and current from both the panels were measured for different inclinations. The absolute power output was calculated simply by multiplying the voltage and the current:

$$P = U \cdot I = 9{,}02V \cdot 0{,}01333A = 0{,}12024W \rightarrow 120{,}24mW \tag{3.13}$$

The measured and the calculated values can be found for the monocrystalline panel in Appendix VI on page 55 and for the polycrystalline in Appendix VII on page 57. The values in the above example are colored in Appendix VI.

So that the panels could be compared, it is necessary to calculate a relative value from the absolute values. It is done by comparing every value with the maximal measured or calculated value, separately for the respective panel. The following values in the examples are colored in Appendix VI.

A relative value for voltage is calculated by:

$$U_{\%} = \frac{U}{U_{max}} \cdot 100\% = \frac{9{,}02V}{16{,}42V} \cdot 100\% = 54{,}93\% \tag{3.14}$$

A relative value for current is calculated by:

$$I_{\%} = \frac{I}{I_{max}} \cdot 100\% = \frac{0{,}01333A}{0{,}01446A} \cdot 100\% = 92{,}19\% \tag{3.15}$$

A relative value for power is calculated by:

$$P_{\%} = \frac{P}{P_{max}} \cdot 100\% = \frac{0{,}12024W}{0{,}14504W} \cdot 100\% = 82{,}90\% \tag{3.16}$$

Next, the results are plotted:

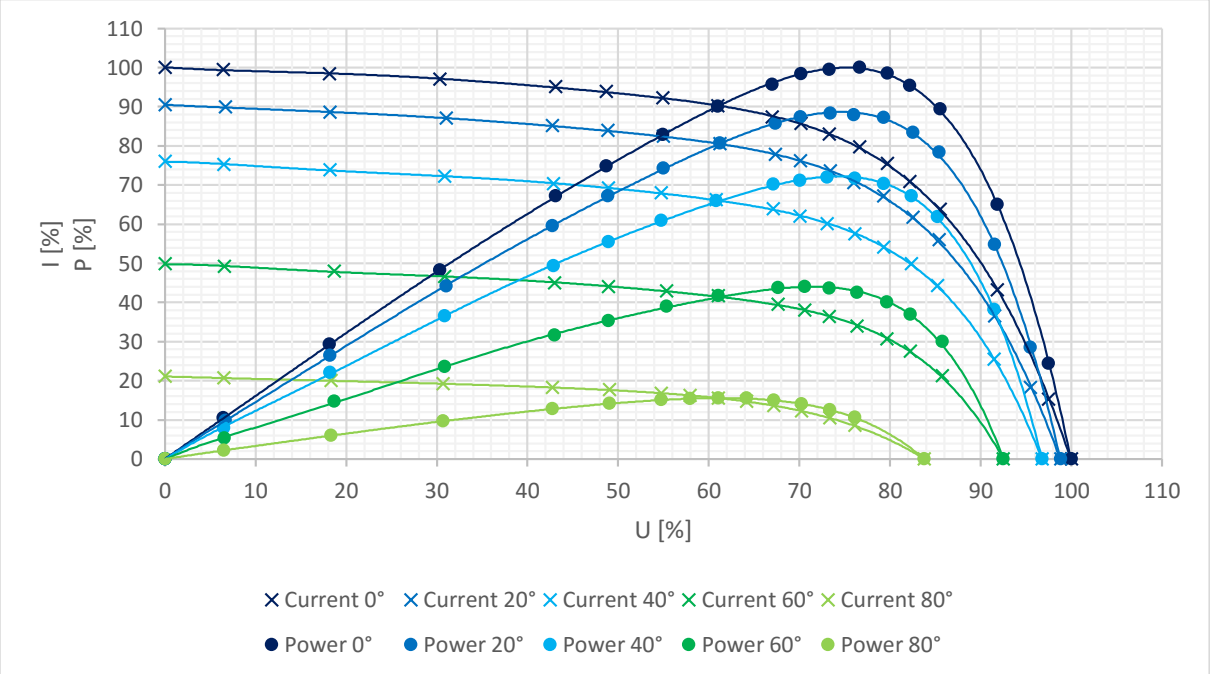

Figure 3.11 – Plot of V-A- and power characteristics of monocrystalline PV panel Siemens T10 for different inclinations

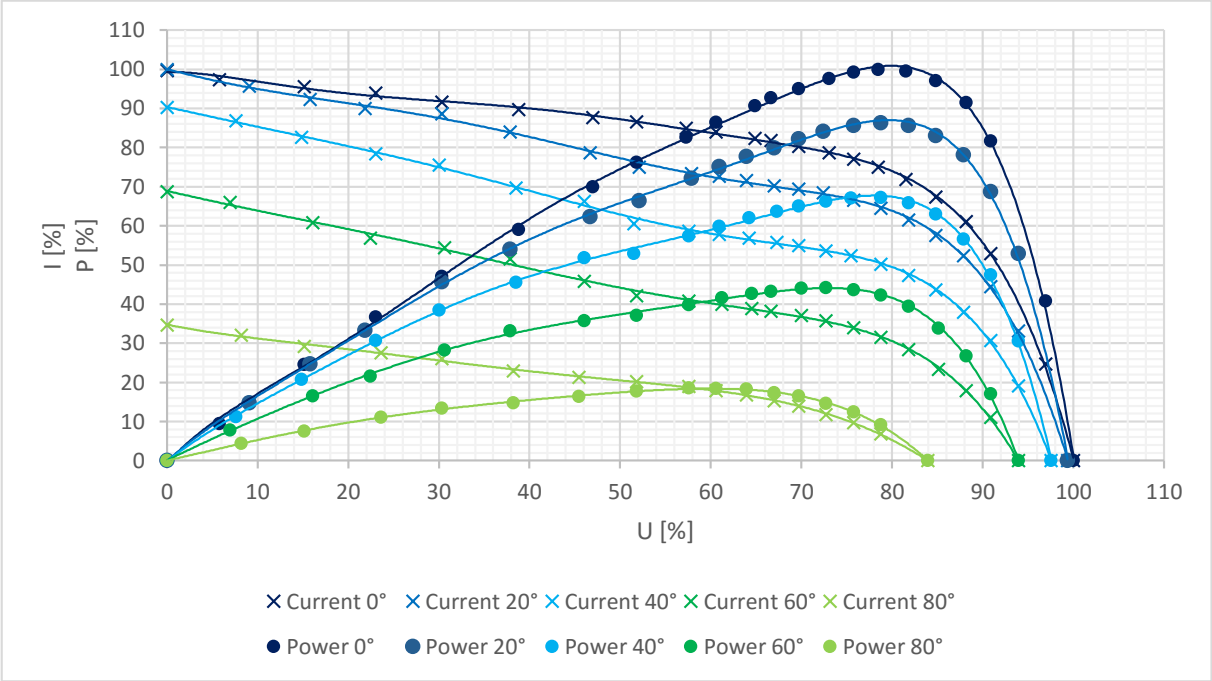

Figure 3.12 – Plot of V-A- and power characteristics of polycrystalline PV panel Schott Poly 165 for different inclinations

Efficiency is calculated for both of the panels for an inclination angle of 0°. The area of the panels are first calculated. Area of the monocrystalline panel:

$$A_{mono} = 0{,}31m \cdot 0{,}63m = 0{,}195m^2 \tag{3.17}$$

Area of the polycrystalline panel:

$$A_{poly} = 1{,}53m \cdot 0{,}76m = 1{,}16m^2 \tag{3.18}$$

Efficiency of the monocrystalline panel. P_{mpp} is found from Appendix VI:

$$\eta_{mono} = \frac{U_{mpp} \cdot I_{mpp}}{E_{mono} \cdot A_{mono}} \cdot 100\% = \frac{P_{mpp}}{E_{mono} \cdot A_{mono}} \cdot 100\% = \frac{0{,}14504W}{7{,}7W \cdot m^{-2} \cdot 0{,}195m^2} \cdot 100\% = 9{,}66\% \tag{3.19}$$

Efficiency of the polycrystalline panel. P_{mpp} can be found from Appendix VII:

$$\eta_{poly} = \frac{U_{mpp} \cdot I_{mpp}}{E_{poly} \cdot A_{poly}} \cdot 100\% = \frac{P_{mpp}}{E_{poly} \cdot A_{poly}} \cdot 100\% = \frac{0{,}73815W}{2{,}7W \cdot m^{-2} \cdot 1{,}16m^2} \cdot 100\% = 23{,}57\% \tag{3.20}$$

It is also possible to calculate the theoretical efficiencies of the panels from the information we know from the manufacturer. The theoretical efficiency for the monocrystalline panel:

$$\eta_{mono,t} = \frac{P_{mpp,t}}{E_t \cdot A_{mono}} \cdot 100\% = \frac{10W}{1000W \cdot m^{-2} \cdot 0{,}195m^2} \cdot 100\% = 5{,}13\% \tag{3.21}$$

The theoretical efficiency of the polycrystalline panel:

$$\eta_{poly,t} = \frac{P_{mpp,t}}{E_t \cdot A_{poly}} \cdot 100\% = \frac{165{,}0W}{1000W \cdot m^{-2} \cdot 1{,}16m^2} \cdot 100\% = 14{,}22\% \quad (3.22)$$

Conclusion

No great differences are found in the relative power output between the two panels, as seen in Figure 3.11 and Figure 3.12. Theoretically the monocrystalline panel should be more sensitive to an inclination than the polycrystalline panel. The reason to that this difference is not seen, might lay in the fact that the irradiance was really low during the measurements.

The V-A characteristics of the monocrystalline panel shows expected shapes. The characteristics of the polycrystalline panel on the other hand has unexpected shapes for voltages under 60 % of the maximal voltage. Above 60 % the V-A characteristics are smooth, as they should be. The reason for these unexpected shapes might lay in the fact that the irradiance was unevenly distributed across the panel.

For both panels, the efficiencies that were calculated from the measured values, were lot higher than the theoretical efficiencies that were calculated from the information given by the manufacturer. Most likely the reason for this is the same as in the measurement in Chapter 3.1.1, that the measured irradiance is not precise enough and that the value for irradiance in the calculations affect the result significantly. It was also noted that the difference between the maximal and the minimal measured irradiance for the monocrystalline panel was about 1,4 W/m^2 and for the polycrystalline about 1,0 W/m^2. These values are great compared to the irradiances that were measured and therefore it is very likely that the used values for irradiances in the calculations are wrong. Since light bulbs were used to irradiate the panels it is also likely that there exist an error in the fact that point-like light sources were used to irradiate a large panel from a relatively short distance.

CONCLUSION

Photovoltaic techniques have developed a lot during the last five years. We have seen increasing efficiencies and falling production costs. We have also seen new ideas on the market with different ideas of how to install photovoltaics in more creative ways.

A great example of the rapid growth of photovoltaics can be seen in India, where in 2010, 15 MW of solar power capacity was installed in form of solar panels. Today, in 2016, the capacity lays at 5 000 MW and the goal is to reach 100 000 MW until 2022 so that the energy demand could be met (18). India also has excellent weather conditions for solar power. The sun shines throughout the year and there are about 300 sunny days in a year.

In Finland the conditions for solar power are not that extraordinary as already discussed earlier. Even the bad weather conditions and Finland's northern position, it is becoming more profitable to use solar power due to the dropping production costs. Few simple things also make it possible to generate relatively lot of power with photovoltaics during the winter. Moving the photovoltaics into a winter position where they are faced towards the horizon, increases the power generation significantly. It is also possible to install reflective disks above the photovoltaics to increase the irradiance to the panels.

An interesting example of this can be seen in an article published in YLE Uutiset (19), the Finnish broadcasting company, where Kyösti Iitti says that if solar panels are moved into a winter position they generate about 50 percent of the power that is generated during the summer. This is significantly more than what is claimed by experts, he says. His house is not connected to the power grid but is powered completely by 20 solar panels. He also has a diesel generator in his basement in case the photovoltaics would not generate enough power during the darkest winter times. He still aims to use as little electricity as possible. The house is heated by a fireplace and he uses only a wooden heated oven, but all other home appliances, such as the washing machine and the dishwasher, are operated with the power that is generated with the photovoltaics. It is interesting to see from this example that even in Finland it is possible to generate almost all the needed power for a small household with only photovoltaics.

Even though photovoltaics are getting more common, there are still great challenges that are to be faced. The low efficiencies and the problem of effective energy storage are the central challenges concerning photovoltaic systems. If techniques to increase the efficiency of solar power would be found, the energy production would be revolutionized since the radiated energy from the sun to the earth is so much larger than our energy needs.

It is still to be seen how much renewables and solar power will grow in the future, but the expectations are high.

REFERENCES

1. **Energiateollisuus ry.** Vesivoima. [Online] 2015. http://energia.fi/energia-ja-ymparisto/energialahteet/vesivoima.

2. **Janíček, et al.** *Renewable Energy Sources 1, Technologies for a Sustainable Future.* Bratislava : s.n., 2009.

3. **Keyhani, Ali.** *Design of Smart Power Grid Renewable Energy Systems.* Hoboken, New Jersey : John Wiley & Sons, Inc., 2011.

4. **REN21 - Renewable Energy Policy Network for the 21st Century.** *Renewables 2015, Global Status Report.* Paris : REN21 Secretariat, 2015.

5. **U.S. Energy Information Administration.** International Energy Statistics. [Online] 2015. http://www.eia.gov/cfapps/ipdbproject/iedindex3.cfm?tid=2&pid=2&aid=7&cid=regions&syid=2000&eyid=2012&unit=MK.

6. **Energiateollisuus ry.** Sähköntuotanto. [Online] 2015. http://energia.fi/energia-ja-ymparisto/sahkontuotanto.

7. **Blencowe, Annette.** Suomi saavutti EU:n uusiutuvan energian tavoitteen kuusi vuotta etuajassa. *YLE Uutiset.* [Online] 26 January 2016. http://yle.fi/uutiset/suomi_saavutti_eun_uusiutuvan_energian_tavoitteen_kuusi_vuotta_etuajassa/8622550.

8. **Energiateollisuus ry.** Aurinkoenergia. [Online] 2015. http://energia.fi/energia-ja-ymparisto/energialahteet/aurinkoenergia.

9. **Koistinen, Antti.** Energiateesit kansanedustajilta: Kivihiili pannaan ja maanteille 200 000 sähköautoa. *YLE Uutiset.* [Online] 8 November 2015. http://yle.fi/uutiset/energiateesit_kansanedustajilta_kivihiili_pannaan_ja_maanteille_200_000_sahkoautoa/8436412.

10. **Lehto, Ina.** Sähköntuotantolaitoksen liittäminen jakeluverkkoon. [Online] 16 12 2011. http://energia.fi/sites/default/files/ohje_tuotannon_liittamisesta_jakeluverkkoon.pdf.

11. **IRENA - International Renewable Energy Agency.** *Renewable Energy Technologies: Cost Analysis Series, Volume 1: Power Sector, Issue 2/5, Concentrating Solar Power.* s.l. : IRENA, 2012.

12. **IEA-ETSAP and IRENA.** Concentrating Solar Power, Technology Brief. [Online] 2013. www.irena.org/Publications.

13. **Luque, Antonio and Hegedus, Steven.** *Handbook of Photovoltaic Science and Engineering, Second Edition.* United Kingdom : John Wiley & Sons Ltd, 2011.

14. **Bollen, Math and Hassan, Fainan.** *Integration of Distributed Generation in the Power System.* Hoboken, New Jersey : John Wiley & Sons, Inc., 2011.

15. **PVEDUCATION.ORG.** Sun Position Calculator. [Online] 2015. http://www.pveducation.org/pvcdrom/properties-of-sunlight/sun-position-calculator.

16. **Hassan, Fainan and Bollen, Math.** *Integration of Distributed Generation in the Power System.* Hoboken, New Jersey : John Wiley & Sons, Inc., 2011.

17. **en:user:Deglr6328.** Wikimedia Commons. *File:Fluorescent lighting spectrum peaks labelled.svg.* [Online] 16 September 2015. https://commons.wikimedia.org/wiki/File:Fluorescent_lighting_spectrum_peaks_labelled.svg.

18. **Koistinen, Antti.** Yle Intiassa: Aurinkoenergiaa rakennetaan sadan ydinvoimalan verran – Fortum kärkkyy uutta kasvua. *YLE Uutiset.* [Online] 21 February 2016. http://yle.fi/uutiset/yle_intiassa_aurinkoenergiaa_rakennetaan_sadan_ydinvoimalan_verran__fortum_karkkyy_uutta_kasvua/8662503.

19. **Mäkelä, Kalle.** Aurinkopaneelin asento ratkaisee – pöytyäläisen Pelle Pelottoman koti saa talvellakin virtaa auringosta. *YLE Uutiset.* [Online] 8 February 2016. http://yle.fi/uutiset/aurinkopaneelin_asento_ratkaisee__poytyalaisen_pelle_pelottoman_koti_saa_talvellakin_virtansa_auringosta/8653004.

APPENDICES

Appendix I – Solar cell SM330 series connection measurement results 49
Appendix II – Solar cell SM330 parallel connection measurement results 50
Appendix III – Solar cell SM330 light spectrum influences measurement results 51
Appendix IV – Solar cell SM330 load resistor size calculation results 53
Appendix V – Solar cell SM330 load resistor size results plot 54
Appendix VI – Solar panel SIEMENS T10 measurement results 55
Appendix VII – Solar panel SCHOTT POLY 165 measurement results 57
Appendix VIII – Solar cell SM330 laboratory measurement for students 59

Appendix I – Solar cell SM330 series connection measurement results

Radiation angle 0°			Radiation angle 20°			Radiation angle 40°		
U [mV]	I [mA]	P [mW]	U [mV]	I [mA]	P [mW]	U [mV]	I [mA]	P [mW]
0,00	17,85	0,00	0,00	16,46	0,00	0,00	13,46	0,00
97,00	17,76	1,72	115,00	16,34	1,88	114,00	13,39	1,53
211,00	17,55	3,70	198,00	16,25	3,22	200,00	13,31	2,66
308,00	17,25	5,31	294,00	16,06	4,72	310,00	13,15	4,08
403,00	16,76	6,75	401,00	15,66	6,28	403,00	12,85	5,18
500,00	15,86	7,93	508,00	14,84	7,54	496,00	12,34	6,12
595,00	14,44	8,59	609,00	13,42	8,17	606,00	11,26	6,82
696,00	12,10	8,42	701,00	11,37	7,97	705,00	9,46	6,67
801,00	8,67	6,94	798,00	8,33	6,65	807,00	6,71	5,41
899,00	4,74	4,26	899,00	4,40	3,96	895,00	3,61	3,23
950,00	2,48	2,36	950,00	2,21	2,10	928,00	2,33	2,16
1008,00	0,00	0,00	1000,00	0,00	0,00	983,00	0,00	0,00

Radiation angle 60°			Radiation angle 80°		
U [mV]	I [mA]	P [mW]	U [mV]	I [mA]	P [mW]
0,00	9,36	0,00	0,00	3,71	0,00
112,00	9,26	1,04	109,00	3,64	0,40
206,00	9,17	1,89	206,00	3,58	0,74
296,00	9,05	2,68	300,00	3,49	1,05
400,00	8,83	3,53	406,00	3,34	1,36
506,00	8,47	4,29	506,00	3,12	1,58
595,00	7,90	4,70	603,00	2,75	1,66
707,00	6,61	4,67	701,00	2,12	1,49
797,00	4,86	3,87	750,00	1,64	1,23
851,00	3,44	2,93	776,00	1,33	1,03
900,00	1,93	1,74	856,00	0,00	0,00
953,00	0,00	0,00			

Appendix II – Solar cell SM330 parallel connection measurement results

Radiation angle 0°			Radiation angle 20°			Radiation angle 40°		
U [mV]	I [mA]	P [mW]	U [mV]	I [mA]	P [mW]	U [mV]	I [mA]	P [mW]
0,00	35,00	0,00	0,00	33,00	0,00	0,00	27,90	0,00
42,00	34,60	1,45	48,00	32,90	1,58	65,00	27,50	1,79
104,00	33,60	3,49	100,00	32,20	3,22	101,00	27,00	2,73
151,00	32,20	4,86	150,00	30,80	4,62	154,00	26,10	4,02
204,00	29,70	6,06	192,00	29,20	5,61	205,00	24,60	5,04
254,00	26,50	6,73	259,00	25,10	6,50	249,00	22,60	5,63
301,00	22,40	6,74	302,00	21,60	6,52	304,00	19,10	5,81
352,00	17,50	6,16	355,00	16,60	5,89	350,00	15,30	5,36
401,00	12,20	4,89	407,00	11,00	4,48	406,00	9,80	3,98
449,00	6,50	2,92	450,00	6,00	2,70	450,00	5,00	2,25
472,00	3,80	1,79	500,00	0,00	0,00	493,00	0,00	0,00
505,00	0,00	0,00						

Radiation angle 60°			Radiation angle 80°		
U [mV]	I [mA]	P [mW]	U [mV]	I [mA]	P [mW]
0,00	18,00	0,00	0,00	8,42	0,00
45,00	17,50	0,79	55,00	8,23	0,45
104,00	16,28	1,69	100,00	7,99	0,80
151,00	15,00	2,27	151,00	7,58	1,14
201,00	13,28	2,67	208,00	6,87	1,43
251,00	11,30	2,84	252,00	6,11	1,54
308,00	8,79	2,71	297,00	5,06	1,50
351,00	6,66	2,34	350,00	3,47	1,21
400,00	4,20	1,68	396,00	1,76	0,70
440,00	2,09	0,92	438,00	0,00	0,00
478,00	0,00	0,00			

Appendix III – Solar cell SM330 light spectrum influences measurement results

Incandescent, 60W						Incandescent, 150W					
Absolute values			Relative values			Absolute values			Relative values		
U [mV]	I [mA]	P [mW]	$U_{\%}$ [%]	P_{rel} [-]	$P_{\%}$ [%]	U [mV]	I [mA]	P [mW]	$U_{\%}$ [%]	P_{rel} [-]	$P_{\%}$ [%]
0	18,75	0,00	0,00	0,000	0,00	0	52,70	0,00	0,00	0,000	0,00
103	18,71	1,93	10,03	0,071	20,69	104	53,20	5,53	9,55	0,071	20,55
212	18,57	3,94	20,64	0,145	42,27	213	53,00	11,29	19,56	0,144	41,92
308	18,34	5,65	29,99	0,208	60,65	305	52,50	16,01	28,01	0,204	59,46
393	17,96	7,06	38,27	0,260	75,79	408	51,30	20,93	37,47	0,267	77,73
506	17,02	8,61	49,27	0,318	92,47	503	48,80	24,55	46,19	0,313	91,16
602	15,47	9,31	58,62	0,343	100,00	604	43,90	26,52	55,46	0,338	98,47
698	13,18	9,20	67,96	0,339	98,78	705	36,70	25,87	64,74	0,330	96,08
803	9,62	7,72	78,19	0,285	82,95	805	27,60	22,22	73,92	0,283	82,51
907	5,36	4,86	88,32	0,179	52,20	906	17,10	15,49	83,20	0,198	57,53
1027	0,00	0,00	100,00	0,000	0,00	1003	6,60	6,62	92,10	0,084	24,58
						1089	0,00	0,00	100,00	0,000	0,00

LED, PILA, 9,5W						LED, PHILIPS Fortimo, 45W					
Absolute values			Relative values			Absolute values			Relative values		
U [mV]	I [mA]	P [mW]	$U_{\%}$ [%]	P_{rel} [-]	$P_{\%}$ [%]	U [mV]	I [mA]	P [mW]	$U_{\%}$ [%]	P_{rel} [-]	$P_{\%}$ [%]
0	2,56	0,00	0,00	0,000	0,00	0	50,00	0,00	0,00	0,000	0,00
106	2,49	0,26	13,01	0,019	5,68	102	49,70	5,07	9,40	0,018	5,13
195	2,43	0,47	23,93	0,035	10,19	196	49,50	9,70	18,06	0,034	9,81
251	2,38	0,60	30,80	0,044	12,85	309	49,10	15,17	28,48	0,053	15,34
302	2,33	0,70	37,06	0,052	15,14	402	48,30	19,42	37,05	0,067	19,63
345	2,27	0,78	42,33	0,058	16,85	509	46,30	23,57	46,91	0,082	23,83
396	2,20	0,87	48,59	0,064	18,74	608	42,50	25,84	56,04	0,090	26,13
452	2,10	0,95	55,46	0,070	20,42	703	36,70	25,80	64,79	0,090	26,09
505	1,99	1,00	61,96	0,074	21,62	806	28,40	22,89	74,29	0,079	23,14
548	1,86	1,02	67,24	0,075	21,92	899	19,60	17,62	82,86	0,061	17,82
600	1,67	1,00	73,62	0,074	21,55	1004	8,80	8,84	92,53	0,031	8,93
704	1,07	0,75	86,38	0,056	16,20	1085	0,00	0,00	100,00	0,000	0,00
815	0,00	0,00	100,00	0,000	0,00						

Fluorescent, room						Fluorescent, PHILIPS Genie 11W					
Absolute values			Relative values			Absolute values			Relative values		
U [mV]	I [mA]	P [mW]	$U_{\%}$ [%]	P_{rel} [-]	$P_{\%}$ [%]	U [mV]	I [mA]	P [mW]	$U_{\%}$ [%]	P_{rel} [-]	$P_{\%}$ [%]
0	1,20	0,00	0,00	0,000	0,00	0	1,92	0,00	0,00	0,000	0,00
97	1,15	0,11	13,92	0,016	4,75	50	1,87	0,09	6,61	0,010	2,81
204	1,10	0,22	29,27	0,033	9,55	103	1,85	0,19	13,61	0,020	5,73

248	1,06	0,26	35,58	0,038	11,18	150	1,82	0,27	19,82	0,028	8,21
306	1,01	0,31	43,90	0,045	13,15	205	1,78	0,36	27,08	0,038	10,98
349	0,97	0,34	50,07	0,049	14,40	252	1,74	0,44	33,29	0,045	13,19
407	0,90	0,37	58,39	0,054	15,58	305	1,68	0,51	40,29	0,053	15,42
451	0,82	0,37	64,71	0,054	15,73	399	1,57	0,63	52,71	0,065	18,85
497	0,71	0,35	71,31	0,052	15,01	455	1,48	0,67	60,11	0,070	20,26
549	0,57	0,31	78,77	0,046	13,31	507	1,36	0,69	66,97	0,071	20,74
608	0,37	0,22	87,23	0,033	9,57	553	1,23	0,68	73,05	0,070	20,46
654	0,17	0,11	93,83	0,016	4,73	598	1,07	0,64	79,00	0,066	19,25
697	0,00	0,00	100,00	0,000	0,00	652	0,82	0,53	86,13	0,055	16,08
						698	0,54	0,38	92,21	0,039	11,34
						757	0,00	0,00	100,00	0,000	0,00

Appendix IV – Solar cell SM330 load resistor size calculation results

Series connection				Parallel connection			
U [mV]	**I [mA]**	**P [mW]**	**R [Ω]**	**U [mV]**	**I [mA]**	**P [mW]**	**R [Ω]**
0,00	17,85	0,00	0,00	0,00	35,00	0,00	0,00
97,00	17,76	1,72	5,46	42,00	34,60	1,45	1,21
211,00	17,55	3,70	12,02	104,00	33,60	3,49	3,10
308,00	17,25	5,31	17,86	151,00	32,20	4,86	4,69
403,00	16,76	6,75	24,05	204,00	29,70	6,06	6,87
500,00	15,86	7,93	31,53	254,00	26,50	6,73	9,58
595,00	14,44	8,59	41,20	301,00	22,40	6,74	13,44
696,00	12,10	8,42	57,52	352,00	17,50	6,16	20,11
801,00	8,67	6,94	92,39	401,00	12,20	4,89	32,87
899,00	4,74	4,26	189,66	449,00	6,50	2,92	69,08
950,00	2,48	2,36	383,06	472,00	3,80	1,79	124,21
1008,00	0,00	0,00	∞	505,00	0,00	0,00	∞

Appendix V – Solar cell SM330 load resistor size results plot

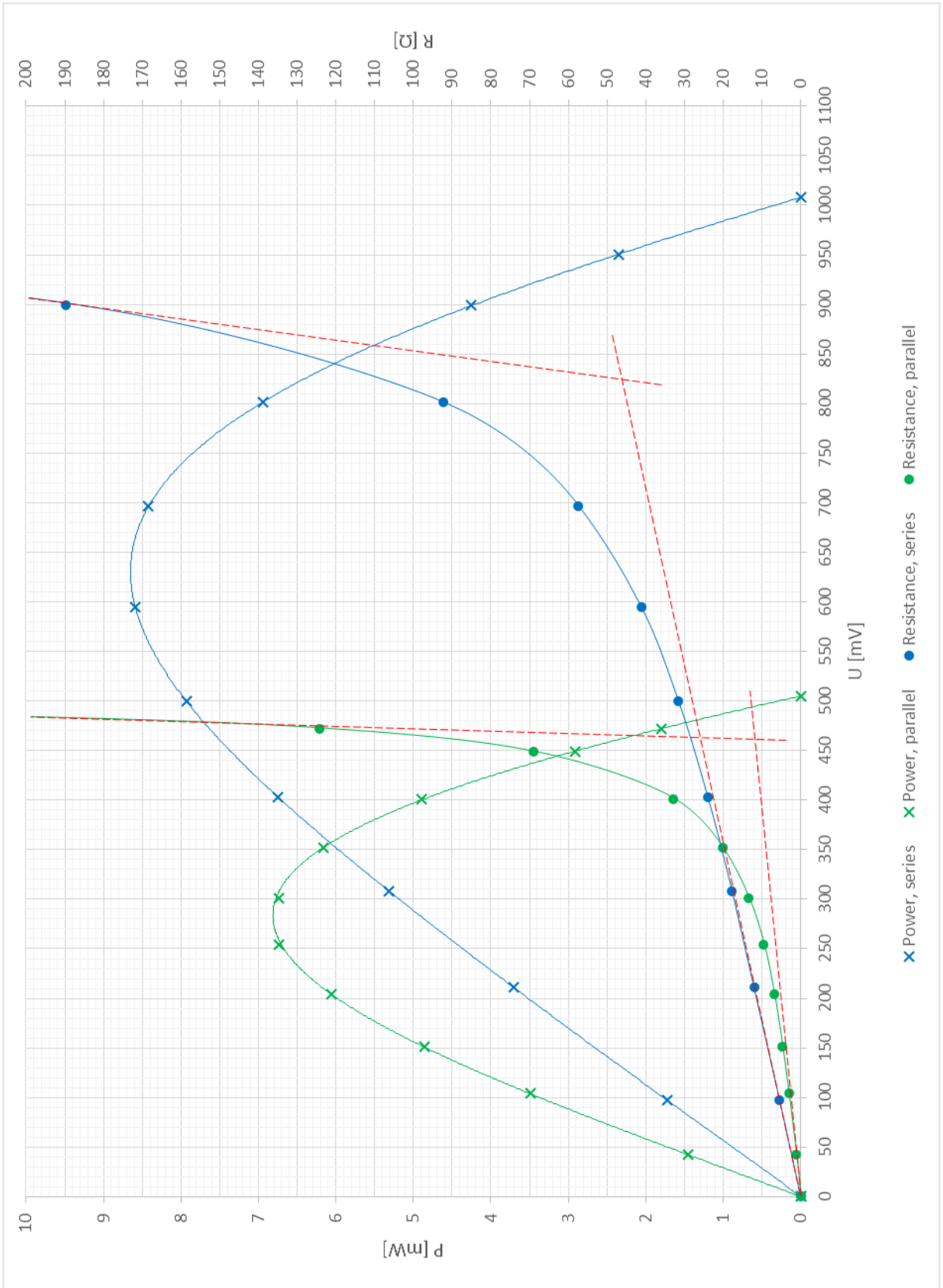

Appendix VI – Solar panel SIEMENS T10 measurement results

Radiation angle 0°						Radiation angle 20°					
Absolute values			Relative values			Absolute values			Relative values		
U [V]	I [mA]	P [mW]	$U_{\%}$ [%]	$I_{\%}$ [%]	$P_{\%}$ [%]	U [V]	I [mA]	P [mW]	$U_{\%}$ [%]	$I_{\%}$ [%]	$P_{\%}$ [%]
0,00	14,46	0,00	0,00	100,00	0,00	0,00	13,08	0,00	0,00	90,46	0,00
1,05	14,39	15,11	6,39	99,52	10,42	1,09	13,00	14,17	6,64	89,90	9,77
2,98	14,23	42,41	18,15	98,41	29,24	2,99	12,81	38,30	18,21	88,59	26,41
4,98	14,03	69,87	30,33	97,03	48,17	5,09	12,58	64,03	31,00	87,00	44,15
7,08	13,75	97,35	43,12	95,09	67,12	7,02	12,31	86,42	42,75	85,13	59,58
7,99	13,58	108,50	48,66	93,91	74,81	8,02	12,14	97,36	48,84	83,96	67,13
9,02	13,33	120,24	54,93	92,19	82,90	9,03	11,92	107,64	54,99	82,43	74,21
10,01	13,04	130,53	60,96	90,18	90,00	10,05	11,64	116,98	61,21	80,50	80,66
11,00	12,62	138,82	66,99	87,28	95,71	11,06	11,24	124,31	67,36	77,73	85,71
11,52	12,39	142,73	70,16	85,68	98,41	11,51	11,01	126,73	70,10	76,14	87,37
12,03	11,99	144,24	73,26	82,92	99,45	12,05	10,63	128,09	73,39	73,51	88,32
12,59	11,52	145,04	76,67	79,67	100,00	12,48	10,21	127,42	76,00	70,61	87,85
13,09	10,91	142,81	79,72	75,45	98,47	13,02	9,72	126,55	79,29	67,22	87,26
13,49	10,25	138,27	82,16	70,89	95,34	13,55	8,92	120,87	82,52	61,69	83,33
14,05	9,22	129,54	85,57	63,76	89,32	14,03	8,10	113,64	85,44	56,02	78,35
15,08	6,25	94,25	91,84	43,22	64,98	15,03	5,28	79,36	91,53	36,51	54,72
16,01	2,21	35,38	97,50	15,28	24,40	15,68	2,63	41,24	95,49	18,19	28,43
16,42	0,00	0,00	100,00	0,00	0,00	16,23	0,00	0,00	98,84	0,00	0,00

Radiation angle 40°						Radiation angle 60°					
Absolute values			Relative values			Absolute values			Relative values		
U [V]	I [mA]	P [mW]	$U_{\%}$ [%]	$I_{\%}$ [%]	$P_{\%}$ [%]	U [V]	I [mA]	P [mW]	$U_{\%}$ [%]	$I_{\%}$ [%]	$P_{\%}$ [%]
0,00	10,99	0,00	0,00	76,00	0,00	0,00	7,20	0,00	0,00	49,79	0,00
1,06	10,88	11,53	6,46	75,24	7,95	1,07	7,11	7,61	6,52	49,17	5,25
2,99	10,68	31,93	18,21	73,86	22,02	3,06	6,94	21,24	18,64	47,99	14,64
5,07	10,44	52,93	30,88	72,20	36,49	5,07	6,74	34,17	30,88	46,61	23,56
7,04	10,17	71,60	42,87	70,33	49,36	7,06	6,50	45,89	43,00	44,95	31,64
8,03	10,01	80,38	48,90	69,23	55,42	8,03	6,37	51,15	48,90	44,05	35,27
8,99	9,83	88,37	54,75	67,98	60,93	9,09	6,21	56,45	55,36	42,95	38,92
9,99	9,58	95,70	60,84	66,25	65,99	10,02	6,03	60,42	61,02	41,70	41,66
11,02	9,23	101,71	67,11	63,83	70,13	11,11	5,71	63,44	67,66	39,49	43,74
11,50	8,97	103,16	70,04	62,03	71,12	11,59	5,50	63,75	70,58	38,04	43,95
12,00	8,69	104,28	73,08	60,10	71,90	12,03	5,26	63,28	73,26	36,38	43,63
12,50	8,32	104,00	76,13	57,54	71,71	12,54	4,91	61,57	76,37	33,96	42,45
13,02	7,83	101,95	79,29	54,15	70,29	13,08	4,44	58,08	79,66	30,71	40,04
13,52	7,21	97,48	82,34	49,86	67,21	13,50	3,97	53,60	82,22	27,46	36,95
14,00	6,41	89,74	85,26	44,33	61,87	14,08	3,08	43,37	85,75	21,30	29,90

15,02	3,68	55,27	91,47	25,45	38,11	15,19	0,00	0,00	92,51	0,00	0,00
15,89	0,00	0,00	96,77	0,00	0,00						

Radiation angle 80°					
Absolute values			**Relative values**		
U [V]	**I [mA]**	**P [mW]**	**$U_{\%}$ [%]**	**$I_{\%}$ [%]**	**$P_{\%}$ [%]**
0,00	3,05	0,00	0,00	21,09	0,00
1,06	2,99	3,17	6,46	20,68	2,19
3,01	2,89	8,70	18,33	19,99	6,00
5,04	2,78	14,01	30,69	19,23	9,66
7,02	2,64	18,53	42,75	18,26	12,78
8,05	2,55	20,53	49,03	17,63	14,15
8,99	2,43	21,85	54,75	16,80	15,06
9,51	2,35	22,35	57,92	16,25	15,41
10,02	2,25	22,55	61,02	15,56	15,54
10,54	2,13	22,45	64,19	14,73	15,48
11,03	1,97	21,73	67,17	13,62	14,98
11,53	1,77	20,41	70,22	12,24	14,07
12,04	1,51	18,18	73,33	10,44	12,54
12,50	1,23	15,38	76,13	8,51	10,60
13,76	0,00	0,00	83,80	0,00	0,00

Appendix VII – Solar panel SCHOTT POLY 165 measurement results

Radiation angle 0°						Radiation angle 20°					
Absolute values			Relative values			Absolute values			Relative values		
U [V]	I [mA]	P [mW]	$U_{\%}$ [%]	$I_{\%}$ [%]	$P_{\%}$ [%]	U [V]	I [mA]	P [mW]	$U_{\%}$ [%]	$I_{\%}$ [%]	$P_{\%}$ [%]
0,00	37,90	0,00	0,00	99,74	0,00	0,00	38,00	0,00	0,00	100,00	0,00
1,90	37,00	70,30	5,76	97,37	9,52	3,00	36,40	109,20	9,09	95,79	14,79
5,00	36,30	181,50	15,15	95,53	24,59	5,20	35,10	182,52	15,76	92,37	24,73
7,60	35,70	271,32	23,03	93,95	36,76	7,20	34,20	246,24	21,82	90,00	33,36
10,00	34,80	348,00	30,30	91,58	47,14	10,00	33,70	337,00	30,30	88,68	45,65
12,80	34,10	436,48	38,79	89,74	59,13	12,50	31,90	398,75	37,88	83,95	54,02
15,50	33,30	516,15	46,97	87,63	69,92	15,40	29,90	460,46	46,67	78,68	62,38
17,10	32,90	562,59	51,82	86,58	76,22	17,20	28,50	490,20	52,12	75,00	66,41
18,90	32,30	610,47	57,27	85,00	82,70	19,10	27,90	532,89	57,88	73,42	72,19
20,00	31,90	638,00	60,61	83,95	86,43	20,10	27,60	554,76	60,91	72,63	75,16
21,40	31,30	669,82	64,85	82,37	90,74	21,10	27,20	573,92	63,94	71,58	77,75
22,00	31,10	684,20	66,67	81,84	92,69	22,10	26,70	590,07	66,97	70,26	79,94
23,00	30,50	701,50	69,70	80,26	95,03	23,00	26,40	607,20	69,70	69,47	82,26
24,10	29,90	720,59	73,03	78,68	97,62	23,90	26,00	621,40	72,42	68,42	84,18
25,00	29,30	732,50	75,76	77,11	99,23	25,00	25,30	632,50	75,76	66,58	85,69
25,90	28,50	738,15	78,48	75,00	100,00	26,00	24,50	637,00	78,79	64,47	86,30
26,90	27,30	734,37	81,52	71,84	99,49	27,00	23,40	631,80	81,82	61,58	85,59
28,00	25,60	716,80	84,85	67,37	97,11	28,00	21,90	613,20	84,85	57,63	83,07
29,10	23,20	675,12	88,18	61,05	91,46	29,00	19,90	577,10	87,88	52,37	78,18
30,00	20,10	603,00	90,91	52,89	81,69	30,00	16,90	507,00	90,91	44,47	68,69
32,00	9,40	300,80	96,97	24,74	40,75	31,00	12,60	390,60	93,94	33,16	52,92
33,00	0,00	0,00	100,00	0,00	0,00	32,80	0,00	0,00	99,39	0,00	0,00

Radiation angle 40°						Radiation angle 60°					
Absolute values			Relative values			Absolute values			Relative values		
U [V]	I [mA]	P [mW]	$U_{\%}$ [%]	$I_{\%}$ [%]	$P_{\%}$ [%]	U [V]	I [mA]	P [mW]	$U_{\%}$ [%]	$I_{\%}$ [%]	$P_{\%}$ [%]
0,00	34,30	0,00	0,00	90,26	0,00	0,00	26,10	0,00	0,00	68,68	0,00
2,50	33,00	82,50	7,58	86,84	11,18	2,30	25,10	57,73	6,97	66,05	7,82
4,90	31,40	153,86	14,85	82,63	20,84	5,30	23,10	122,43	16,06	60,79	16,59
7,60	29,80	226,48	23,03	78,42	30,68	7,40	21,60	159,84	22,42	56,84	21,65
9,90	28,70	284,13	30,00	75,53	38,49	10,10	20,70	209,07	30,61	54,47	28,32
12,70	26,50	336,55	38,48	69,74	45,59	12,50	19,60	245,00	37,88	51,58	33,19
15,20	25,20	383,04	46,06	66,32	51,89	15,20	17,40	264,48	46,06	45,79	35,83
17,00	23,00	391,00	51,52	60,53	52,97	17,10	16,00	273,60	51,82	42,11	37,07
19,00	22,30	423,70	57,58	58,68	57,40	19,00	15,50	294,50	57,58	40,79	39,90
20,10	22,00	442,20	60,91	57,89	59,91	20,20	15,20	307,04	61,21	40,00	41,60
21,20	21,60	457,92	64,24	56,84	62,04	21,30	14,80	315,24	64,55	38,95	42,71

22,20	21,20	470,64	67,27	55,79	63,76	22,00	14,50	319,00	66,67	38,16	43,22
23,00	20,90	480,70	69,70	55,00	65,12	23,10	14,10	325,71	70,00	37,11	44,13
24,00	20,40	489,60	72,73	53,68	66,33	24,00	13,60	326,40	72,73	35,79	44,22
24,90	19,90	495,51	75,45	52,37	67,13	25,00	12,90	322,50	75,76	33,95	43,69
26,00	19,10	496,60	78,79	50,26	67,28	26,00	12,00	312,00	78,79	31,58	42,27
27,00	18,00	486,00	81,82	47,37	65,84	27,00	10,80	291,60	81,82	28,42	39,50
28,00	16,60	464,80	84,85	43,68	62,97	28,10	8,90	250,09	85,15	23,42	33,88
29,00	14,40	417,60	87,88	37,89	56,57	29,10	6,80	197,88	88,18	17,89	26,81
30,00	11,70	351,00	90,91	30,79	47,55	30,00	4,20	126,00	90,91	11,05	17,07
31,00	7,30	226,30	93,94	19,21	30,66	31,00	0,00	0,00	93,94	0,00	0,00
32,20	0,00	0,00	97,58	0,00	0,00						

Radiation angle 80°					
Absolute values			**Relative values**		
U [V]	**I [mA]**	**P [mW]**	**$U_{\%}$ [%]**	**$I_{\%}$ [%]**	**$P_{\%}$ [%]**
0,00	13,20	0,00	0,00	34,74	0,00
2,70	12,20	32,94	8,18	32,11	4,46
5,00	11,10	55,50	15,15	29,21	7,52
7,80	10,50	81,90	23,64	27,63	11,10
10,00	9,90	99,00	30,30	26,05	13,41
12,60	8,70	109,62	38,18	22,89	14,85
15,00	8,10	121,50	45,45	21,32	16,46
17,10	7,70	131,67	51,82	20,26	17,84
19,00	7,20	136,80	57,58	18,95	18,53
20,00	6,80	136,00	60,61	17,89	18,42
21,10	6,40	135,04	63,94	16,84	18,29
22,10	5,80	128,18	66,97	15,26	17,37
23,00	5,30	121,90	69,70	13,95	16,51
24,00	4,50	108,00	72,73	11,84	14,63
25,00	3,70	92,50	75,76	9,74	12,53
26,00	2,60	67,60	78,79	6,84	9,16
27,70	0,00	0,00	83,94	0,00	0,00

Appendix VIII – Solar cell SM330 laboratory measurement for students

Date:	**Photovoltaic cell SM330**	Name: Login:

Assignment:

1. Measure the irradiance (light intensity) to the cells.
2. Measure volt-ampere characteristics for a series connection of the cells and plot the results I=f(U). Measure for a distance of about 25cm between the lamp and the cells.
3. Calculate the power output for every point of the measured voltages and currents. Plot the results P=f(U).
4. Calculate the efficiency from the measured values and from the values given by the manufacturer of the cells. Compare the results.

Connection diagram:

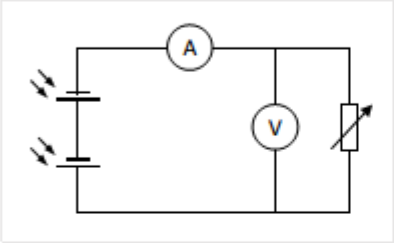

Used apparatus:

Solar cell x2, Monocrystalline SM330

U_{mpp} = 0,5V

I_{mpp} = 330mA

A = $(1{,}09 \cdot 10^{-3})m^2$ x2

Incandescent lamp, 60W

Multimeter x2

Irradiance meter

Variable resistor

Measured values:

Measured irradiance E_m = _____ W/m^2

U_m [mV]	I_m [mA]	P_m [mW]

U_m [mV]	I_m [mA]	P_m [mW]

1

Calculated values:

Power output is calculated for every measured point of voltage and current:

$P_m = U_m \cdot I_m =$

Efficiency is calculated from measured values:

$$\eta_m = \frac{P_{m,max}}{E_m \cdot A} \cdot 100\% =$$

Theoretical efficiency is calculated from the voltage U_{mpp} and current I_{mpp} that generates the highest possible power output according to the manufacturer at an irradiance of $E_t = 1000 W/m^2$ and a temperature of $t = 25°C$:

$$\eta_t = \frac{U_{mpp} \cdot I_{mpp}}{E_t \cdot A} \cdot 100\% =$$

Conclusion: